GLOBAL BIOGEOCHEMICAL CYCLES, VOL. 10, NO. 1, PAGES 89–110, MARCH 1996

On the relations between the oceanic uptake of CO_2 and its carbon isotopes

Martin Heimann and Ernst Maier-Reimer

Max-Planck-Institut für Meteorologie, Hamburg, Germany

Abstract. The recent proposals to estimate the oceanic uptake of CO_2 by monitoring the oceanic change in $^{13}C/^{12}C$ isotope ratio [*Quay et al.*, 1992] or the air-sea $^{13}C/^{12}C$ isotopic disequilibrium [*Tans et al.*, 1993] is reviewed. Because the history of atmospheric CO_2 and $^{13}CO_2$ since preindustrial times is almost the same and increasing in an almost exponential fashion, the oceanic penetration depth of both tracers must be the same. This dynamic constraint permits the establishment of yet a third method to estimate the global ocean uptake of CO_2 from ^{13}C measurements. Using available observations in conjunction with canonical values for global carbon cycle parameters, the three methods yield inconsistent oceanic CO_2 uptake rates for the time period 1970–1990, ranging from 0.6 to 3.1 GtC yr^{-1}. However, uncertainties in the available carbon cycle data must be taken into account. Using a nonlinear estimation procedure, a consistent scenario with an oceanic CO_2 uptake rate of 2.1 ± 0.9 GtC yr^{-1} can be established. The method also permits an investigation of the sensitivities of the different approaches. An analysis of the results of two three-dimensional simulations with the Hamburg model of the oceanic carbon cycle shows that the ^{13}C isotope indeed tracks the oceanic penetration of anthropogenic CO_2. Because of its different time history, bomb produced radiocarbon, as measured at the time of the Geochemical Ocean Sections Study (GEOSECS), correlates not as well to excess carbon.

1. Introduction

Recently, *Quay et al.* [1992, hereafter referred to as QTW] have introduced a new method to determine the oceans uptake of excess CO_2 which is based on observations of changes in oceanic $^{13}C/^{12}C$ stable isotope ratios. The method proceeds by assessing the ^{13}C budget of the combined ocean-atmosphere system. The new element introduced by QTW is an estimate of the change in the oceanic inventory of ^{13}C based on a few measured vertical profiles of the $^{13}C/^{12}C$ ratio obtained during the early 1970s and again 20 years later. This estimate, together with the observed change in atmospheric ^{13}C and the total carbon budget of the atmosphere permits calculation of the ocean uptake of carbon.

At least two major difficulties exist in applying this approach. First, the method requires the determination of the global oceanic change in $^{13}C/^{12}C$ ratio during an extended period of time, necessitating global coverage by surveys at repeated times or the clever use of another tracer such as bomb radiocarbon in order to extrapolate measurements from a few key sites to the global ocean. Second, isotopic ratios of the atmospheric CO_2 sources and sinks have to be specified in order to strike the carbon isotope balance. While $^{13}C/^{12}C$ ratios of fossil fuels are available, this is not the case for CO_2 exchanged with the terrestrial biosphere, primarily because the extent to which the latter is in isotopic disequilibrium with the perturbed atmosphere (the biospheric Suess effect) is not known. As shown below, this leads to considerable uncertainties in the oceanic CO_2 uptake estimates.

The study by QTW has spurred a series of further investigations trying to explore the potential of the stable carbon isotope method. *Tans et al.* [1993, hereafter referred to as TBK] reviewed the ocean-atmosphere isotope balance method of QTW and showed that the requirement for the isotopic measurements in terms of accuracy and calibration are very high. Furthermore, they introduced a second approach to estimate the oceanic uptake of CO_2, which is based on measurements of the isotopic disequilibrium between the air and the surface ocean. In this method one essentially strikes the balance only of the atmospheric CO_2 and ^{13}C reservoirs. This method does not rely on oceanic data at depth, but requires the determination of surface ocean $^{13}C/^{12}C$ isotope ratios. A further advantage of this method is that

Paper number 95GB03191.
0886-6236/96/95GB-03191$10.00

the latter do not have to be monitored with time, but that essentially a single global survey would suffice to determine the air-sea isotopic disequilibrium. On the other hand, as in the ocean-atmosphere budget method of QTW, the unknown isotopic disequilibrium of the terrestrial biosphere carbon pools also enters the resulting balance equation.

Broecker and Peng [1993] also addressed the uncertainties of the method by QTW and discussed the particular role of the biospheric reservoirs. Their essential conclusion is that the information of the $^{13}C/^{12}C$ isotope does not place strong constraints on the current carbon budget of the ocean.

There is an additional piece of information that, so far, has not yet been employed. There exists a dynamic constraint which is imposed because both, atmospheric CO_2 and $^{13}CO_2$, as documented from ice core and atmospheric observations, show, on timescales beyond 10 years, a very similar, almost exponential perturbation history since preindustrial times. This implies, that the oceanic penetration depth of both tracers must be approximately the same. On the basis of this constraint a third method to determine the oceans uptake of anthropogenic CO_2 can be established. Similar to the ocean-atmosphere budget method of QTW, this approach also requires the determination of the globally averaged rate of change of the oceanic $^{13}C/^{12}C$ ratio. However, the unknown Suess effect of the terrestrial biosphere does not enter into the calculation. On the other hand, the knowledge of other carbon cycle parameters is required, in particular, the gross air-sea gas exchange flux and the atmospheric change in $^{13}C/^{12}C$ ratio since preindustrial times.

All three methods, that is, the atmosphere-ocean ^{13}C budget method of QTW, the atmosphere ^{13}C budget method of TBK, and the method based on the aforementioned dynamic constraint are compared in the first part of this paper. Of particular interest is the question, as to which extent the three approaches are compatible with each other? Also of interest is their sensitivity with respect to the uncertainties in the carbon cycle input data.

All three approaches require the determination of globally averaged quantities, such as the rate of change of the oceanic $^{13}C/^{12}C$ isotope ratio. However, the penetration of transient tracers into the ocean exhibits a three-dimensional structure, which must be taken into account when devising a sampling strategy. This structure will depend not only on physical and biological transport within the ocean but also on the details of the input function at the surface and on its temporal evolution in the past.

To address this problem, we illustrate in the second part of the paper the three approaches by means of two simulation experiments using the three-dimensional Hamburg model of the ocean carbon cycle (HAMOCC 3) [*Maier-Reimer*, 1993]. Of particular interest here is the extent to which both carbon isotopes, ^{13}C and bomb radiocarbon, may be used to track the fate of anthropogenic CO_2 in the ocean.

2. Global Analysis

In this section we adopt a global viewpoint. Using the methodology of *Tans* [1980] and TBK, we first outline the derivation of the approaches by QTW and by TBK to estimate the current oceanic CO_2 uptake rate from $^{13}C/^{12}C$ isotope ratio measurements. We refer to the original articles by QTW and TBK for a detailed discussion of the underlying assumptions. In addition, we also include in the analysis an estimate of the contributions due to carbon transport by rivers. Subsequently, using the same notation, we present a derivation of the dynamical constraint method. Finally, we explore the consistency of the three relations and investigate their sensitivity with respect to the carbon cycle input data.

2.1. The Ocean-Atmosphere ^{13}C Budget [*Quay et al.*, 1992]

The method proposed by QTW is derived from the balance of the combined atmosphere-ocean pools, both of total carbon and of the ^{13}C isotope (see Figure 1). For total carbon, this balance is given by

$$\dot{N}_a + \dot{N}_{oc} = Q_{foss} + F_{ba} - F_{ab} + 0.5F_{r,dic} + F_{r,org} \quad (1)$$

where $\dot{N}_a$ and $\dot{N}_{oc}$ denote the rate of change ($\dot{N} = \frac{d}{dt}N$) of carbon in the atmosphere and the ocean, respectively, and Q_{foss} is the fossil fuel CO_2 source. $F_{ba} - F_{ab}$ represents the net carbon flux from the biosphere to the atmosphere, where the symbol F_{ab} denotes the gross flux into the terrestrial biosphere due to photosynthesis and F_{ba} the return flux due to autotrophic and heterotrophic respiration from vegetation, plant litter, and soils. F_{ba} also includes any carbon released from changes in land use, for example, resulting from deforestation in the tropics.

Figure 1 also shows the carbon fluxes induced by carbon transport in rivers [*Sarmiento and Sundquist*, 1992], both in organic ($F_{r,org}$), and inorganic forms ($F_{r,dic}$). Half of the flux of inorganic carbon is assumed to come from CO_2 in soils, while the other half is assumed to be coming from carbonate rocks. If we assume a steady state of the carbonate weathering cycle, then the inorganic carbon river influx must be balanced by formation of carbonate sediments, hence half of the inorganic river carbon is transferred back to the atmosphere as CO_2, while the other half ends up in carbonate sediments and can thus be discounted in (1). The flux of organic carbon is assumed to be of terrestrial biospheric origin. The steady state assumption of the

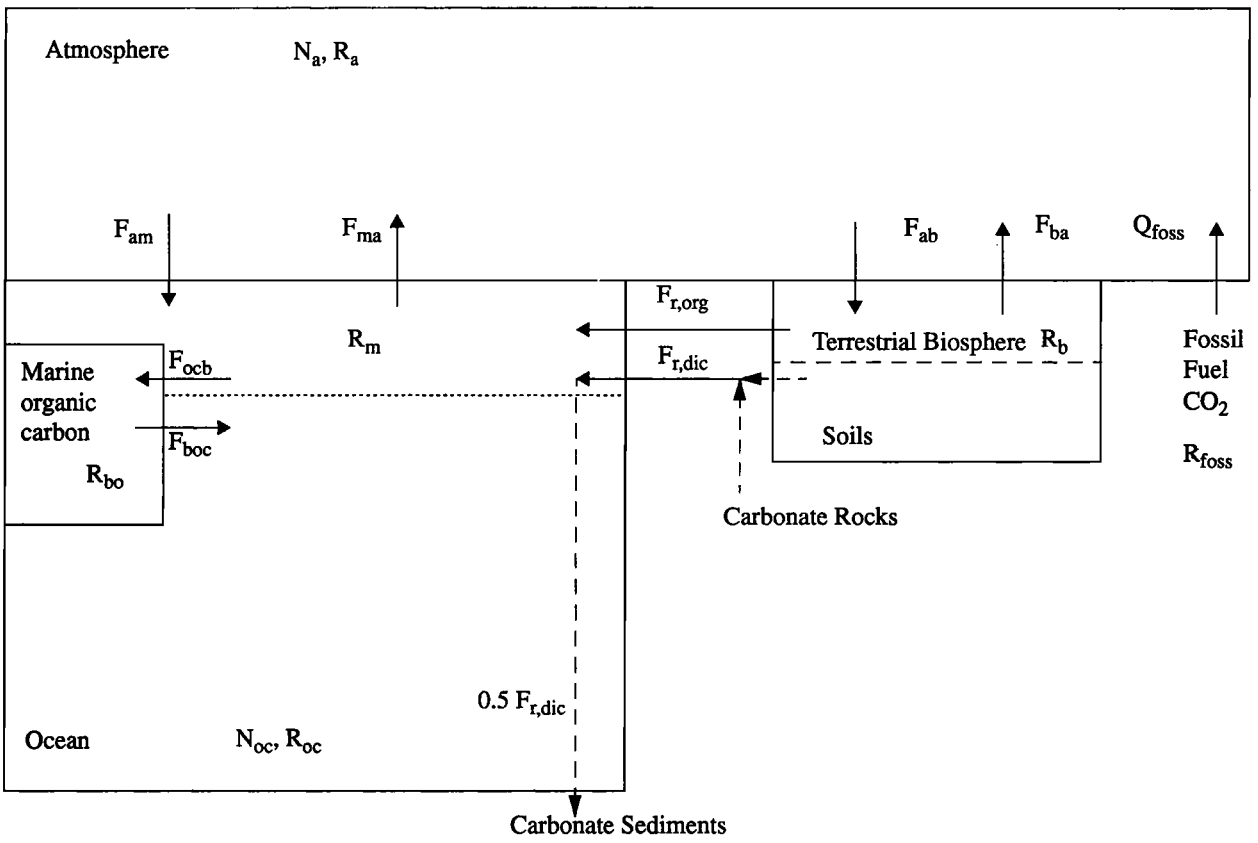

Figure 1. Carbon pools and exchange fluxes.

river carbon transports implies that $0.5F_{r,dic} + F_{r,org}$ must be balanced by a biospheric carbon uptake, that is, by a fraction of $F_{ab} - F_{ba}$.

A similar equation holds for the ^{13}C isotope

$$\frac{d}{dt}(N_a R_a) + \frac{d}{dt}(N_{oc} R_{oc}) = Q_{foss} R_{foss} + F_{ba} R_b - F_{ab} \alpha_{ab} R_a + 0.5 F_{r,dic} R_{r,soil} + F_{r,org} R_{r,org} + F_{boc} R_{ocb} - F_{ocb} \alpha_{ocb} R_m \quad (2)$$

where we denote $^{13}C/^{12}C$ isotopic ratios by the symbol R. R as introduced here is defined as the ratio $^{13}C/(^{12}C + ^{13}C)$, whereas reported measurements commonly refer to the isotope ratio $^{13}C/^{12}C$, but the difference between these two definitions can be neglected in the present context since $^{13}C/^{12}C \sim 0.01$. Isotope ratios usually are reported in the δ notation as relative deviations from the Pee Dee belemite (PDB) standard: $\delta = R/R_{PDB} - 1$ where the δ values are expressed in permil.

Here α_{ab} denotes the fractionation factor for photosynthesis, R_b denotes the average $^{13}C/^{12}C$ isotopic ratio of the CO_2 flux from biosphere to atmosphere, and $R_{r,org}$ denotes the $^{13}C/^{12}C$ ratio of organic river carbon. $R_{r,soil}$ is the isotopic ratio of the soil CO_2 associated in the weathering of carbonate rocks.

The last two terms in (2) denote contributions to the ^{13}C budget resulting from exchanges between the oceanic inorganic and organic carbon pools. These terms have to be included in the budget equation, since the measurements of the oceanic isotopic ratio (R_{oc}) refer only to dissolved inorganic carbon (DIC). We assume that the oceanic organic carbon pool is not changing in size because of nutrient limitation of the marine biosphere [*Broecker*, 1991], hence the exchange fluxes must be equal: $F_{boc} = F_{ocb}$. Here α_{ocb} is the fractionation factor for the formation of organic material of isotopic ratio R_{ocb}, and R_m is the $^{13}C/^{12}C$ ratio of DIC in the surface (mixed) layer, where this formation is assumed to occur. A further term reflecting isotopic exchanges with the oceanic carbonate pool should also be included, however, it is assumed to be rather small and its contribution to the ^{13}C budget may be neglected [TBK].

Similar to the derivation given by TBK, we next define R_{ab}^{eq}, the isotopic ratio of atmospheric gaseous carbon in isotopic equilibrium with the current biosphere:

$$\alpha_{ab} R_{ab}^{eq} = R_b \quad (3)$$

and analogously R^{eq}_{mb}, the isotopic ratio of surface water DIC in isotopic equilibrium with current marine organic carbon:

$$\alpha_{ocb} R^{eq}_{mb} = R_{ocb} \tag{4}$$

Finally, we multiply the total carbon budget (1) by R_b and subtract it from the isotope budget (2). After solving for the oceanic CO_2 uptake rate ($\dot{N}_{oc}$) and making use of the definitions (3) and (4) we get

$$\begin{aligned}\dot{N}_{oc}(R_{oc} - R_b) = \\ & Q_{foss}(R_{foss} - R_b) \\ & - \dot{N}_a(R_a - R_b) - N_a\dot{R}_a - N_{oc}\dot{R}_{oc} \\ & + 0.5F_{r,dic}(R_{r,dic} - R_b) + F_{r,org}(R_{r,org} - R_b) \\ & + F_{ab}\alpha_{ab}(R^{eq}_{ab} - R_a) + F_{ocb}\alpha_{ocb}(R^{eq}_{mb} - R_m)\end{aligned} \tag{5}$$

The crucial quantity appearing on the right-hand side of (5) is the rate of change of the oceanic isotopic composition, $\dot{R}_{oc}$. It has to be determined from repeated measurements of the vertical profile of the $^{13}C/^{12}C$ ratio of DIC. Formally, we may write

$$\begin{aligned} N_{oc}\dot{R}_{oc} &= \int_{A_{oc}} \left[\int_0^{h_d} \dot{R}_{oc}(z) C_{oc}(z) dz \right] dA \\ &\approx A_{oc} C_{oc} \dot{D} \end{aligned} \tag{6}$$

where we have defined

$$\dot{D} = < \int_0^{h_d} \dot{R}_{oc}(z) dz > \tag{7}$$

$C_{oc}(z)$ is the oceanic concentration of DIC as a function of depth, which, in the present context, is approximated as uniform throughout the ocean. The angle brackets denote the horizontal average, A_{oc} denotes the surface of the ocean ($3.5\ 10^{14}$ m^2), and h_d denotes its depth.

Equation (5) can be simplified by approximating the fractionation factors α_{ab} and α_{ocb} with unity. Furthermore, the river terms are very small, because the organic and the inorganic carbon river fluxes, $F_{r,org}$ and $F_{r,dic}$, are only about 0.4 GtC yr^{-1} or less [*Degens et al.*, 1991, *Sarmiento and Sundquist*, 1992], which is much smaller than the other gross fluxes in (5), and second because the isotopic compositions $R_{r,org}$ and of the inorganic carbon from soil CO_2 $R_{r,soil}$, are close to terrestrial biospheric material [*Cerling*, 1984; *Mook*, 1986]. In this equation the river terms can thus be neglected.

Using (6), we obtain the final form

$$\begin{aligned}\dot{N}_{oc}(R_{oc} - R_b) \approx \\ & Q_{foss}(R_{foss} - R_b) \\ & - \dot{N}_a(R_a - R_b) - N_a\dot{R}_a - A_{oc}C_{oc}\dot{D} \\ & + F_{ab}(R^{eq}_{ab} - R_a) + F_{ocb}(R^{eq}_{mb} - R_m)\end{aligned} \tag{8}$$

This is essentially the relation given by QTW (their equation (6)), except for the last term which has been introduced by TBK. This equation may be interpreted as a conservation equation of an isotopic "label" [*Tans*, 1980], defined here as a quantity of carbon times its isotopic composition relative to biospheric carbon and is expressed in units of permil gigatons carbon. With this definition, any net biospheric CO_2 source (i.e., $F_{ba} - F_{ab}$) does not appear in (8) since its "label" equals zero by definition.

The last two terms of (8) describe the effects of the isotopic adjustment fluxes of the combined ocean-atmosphere system with the terrestrial and oceanic organic carbon pools. These adjustment fluxes arise because the organic carbon pools are not in isotopic equilibrium with the current atmosphere and ocean, respectively, as a consequence of the anthropogenic perturbation (the so-called "Suess" effect [*Keeling*, 1980]). This disequilibrium is reflected by the isotopic differences $R^{eq}_{ab} - R_a$ and $R^{eq}_{mb} - R_m$. Because of the heterogenous nature of the organic carbon pools this disequilibrium cannot be measured directly and must be estimated, possibly, by means of a model. Because of the uncertain size of these terms, they introduce a substantial uncertainty into the calculation as illustrated below in section 2.5.

2.2. The ^{13}C Budget of the Atmosphere [*Tans et al.*, 1992]

The method proposed by TBK is similar to QTW, except that the balance of total carbon and of the ^{13}C isotope is expressed only for the atmosphere. Therefore air-sea fluxes of total carbon and of ^{13}C enter the budget equations on the right-hand side.

The equation for total carbon is in this case

$$\dot{N}_a = Q_{foss} + F_{ba} - F_{ab} + F_{ma} - F_{am} \tag{9}$$

F_{ma} and F_{am} denote the gross carbon fluxes from sea to air and from air to sea, respectively. The rate of change of the ocean carbon inventory is then

$$\dot{N}_{oc} = F_{am} - F_{ma} + F_{r,org} + 0.5F_{r,dic} \tag{10}$$

The atmospheric balance equation of the ^{13}C isotope is given by

$$\begin{aligned}\frac{d}{dt}(N_a R_a) &= Q_{foss}R_{foss} \\ &\quad + F_{ba}R_b - F_{ab}\alpha_{ab}R_a \\ &\quad + F_{ma}\alpha_{ma}R_m - F_{am}\alpha_{am}R_a\end{aligned} \tag{11}$$

where we have introduced the kinetic fractionation factors α_{ma} and α_{am}.

We define next R^{eq}_{am}, the $^{13}C/^{12}C$ ratio of air in isotopic equilibrium, with current surface ocean DIC:

$$\alpha_{ma} R_m = \alpha_{am} R^{eq}_{am} \tag{12}$$

With this definition, the air-sea exchange term in the budget equation for ^{13}C may be rewritten as

$$\begin{aligned} & F_{ma}\alpha_{ma}R_m - F_{am}\alpha_{am}R_a \\ &= (F_{ma} - F_{am})\alpha_{ma}R_m + F_{am}\alpha_{am}(R_{am}^{eq} - R_a) \\ &= -(\dot{N}_{oc} - F_{r,org} - 0.5F_{r,dic})\alpha_{ma}R_m \\ &\quad + F_{am}\alpha_{am}(R_{am}^{eq} - R_a) \end{aligned} \tag{13}$$

thereby using (10).

Multiplying (9) by R_b and subtracting it from (11) we get after rearrangement and insertion of (3) and (13)

$$\begin{aligned} & \dot{N}_{oc}(\alpha_{ma}R_m - R_b) = \\ & \quad Q_{foss}(R_{foss} - R_b) - \dot{N}_a(R_a - R_b) - N_a\dot{R}_a \\ & \quad + F_{ab}\alpha_{ab}(R_{ab}^{eq} - R_a) + F_{am}\alpha_{am}(R_{am}^{eq} - R_a) \\ & \quad + F_{r,org}(\alpha_{ma}R_m - R_b) + 0.5F_{r,dic}(\alpha_{ma}R_m - R_b) \end{aligned} \tag{14}$$

The fractionation factors α_{ab} and α_{am} on the right-hand side in the third and fourth line can be approximated by unity, resulting in

$$\begin{aligned} & \dot{N}_{oc}(\alpha_{ma}R_m - R_b) \approx \\ & \quad Q_{foss}(R_{foss} - R_b) - \dot{N}_a(R_a - R_b) - N_a\dot{R}_a \\ & \quad + F_{ab}(R_{ab}^{eq} - R_a) + F_{am}(R_{am}^{eq} - R_a) \\ & \quad + (0.5F_{r,dic} + F_{r,org})(\alpha_{ma}R_m - R_b) \end{aligned} \tag{15}$$

This equation corresponds to (17) given by TBK. It differs from the latter in that TBK approximate R_{foss} with $\alpha_{ab}R_a$ and refer the "isotopic label" to the isotopic ratio of the atmosphere, R_a, whereas here it is defined with respect to biospheric carbon, R_b. Furthermore, (15) includes the correction introduced by accounting for carbon transport by rivers.

Compared to the atmosphere-ocean budget, (8) derived in the previous section, here on the right-hand side the oceanic $^{13}C/^{12}C$ ratio change term ($A_{oc}C_{oc}\dot{D}$), is replaced by the oceanic Suess effect term $F_{am}(R_{am}^{eq} - R_a)$, which describes the "isotopic label" flux induced by the isotopic disequilibrium between air and sea. The difference $R_{am}^{eq} - R_a$ has to be determined as a weighted global average, since the local isotopic composition of air in equilibrium with surface water carbon is a strong function of temperature [*Mook et al.*, 1974] and depends also on the local isotopic composition of surface DIC. Also, the $^{13}C/^{12}C$ ratio of atmospheric CO_2 is not uniform [e.g., *Keeling et al.*, 1989] which has to be taken into account. The weights for the averaging are given by the spatially and temporally varying gas exchange rate. TBK have performed such an analysis and give estimates for the global isotopic disequilibrium between air and sea.

2.3. The Dynamic Constraint

The atmospheric perturbation history of both, CO_2, and of $^{13}CO_2$ have been almost the same. This follows from the fact, that changes in the atmospheric $^{13}C/^{12}C$ ratio since preindustrial times have been less than 2‰, while at the same time the CO_2 concentration has increased by more than 20%. On the basis of this we may assume that the oceanic penetration depths [*Broecker and Peng*, 1982] of both tracer perturbations must be almost the same (Note that this argument refers to the ^{13}C isotope itself and not to the $^{13}C/^{12}C$ ratio which exhibits different dynamics than total carbon). This would be exactly true if the following four conditions were met: (1) if the atmospheric concentration levels of both tracers were following an exact exponential trend with the same time constant, (2) if the gas exchange coefficient and the carbonate chemistry constants were the same for CO_2 and $^{13}CO_2$, (3) if there were no isotopic exchanges between inorganic and organic carbon in the ocean, and (4) if the ocean would represent a passive reservoir with linear, time invariant dynamics.

Assuming that the penetration depths for CO_2 and $^{13}CO_2$ are the same provides a constraint which may be used to derive a third, independent relationship between the ocean carbon uptake rate and $^{13}C/^{12}C$ ratio changes in the ocean: Observations of the $^{13}C/^{12}C$ perturbation changes in the atmosphere and in the ocean provide an estimate of the penetration depth which can then be used to estimate the oceanic total carbon uptake.

In reality the conditions (1)-(4) as stated above are only approximately true. The extent to which this approximation affects the proposed relation is discussed further below.

In order to derive the relationship, we consider a horizontally averaged one-dimensional vertical ocean. We next set up four relations. The first two express the oceanic perturbation balance of total carbon and of ^{13}C. The third and fourth relate the oceanic perturbation inventory of the two tracers to the perturbation concentrations at the ocean surface.

The first equation relates the time rate of change in ocean carbon inventory to the perturbations in the surface gas exchange fluxes of CO_2

$$\dot{N}_{oc} = \Delta F_{am} - \Delta F_{ma} \tag{16}$$

where Δ indicates the perturbation of a variable, for example, $\Delta F_{am} = F_{am} - F_{am0}$ and, the index 0 refers to its preindustrial value.

For the carbon isotope we have a similar equation

$$^{13}\dot{N}_{oc} = \Delta^{13}F_{am} - \Delta^{13}F_{ma} \tag{17}$$

The third relation is obtained by using the definition of the penetration depth, H_{oc}, of total carbon

$$H_{oc} = \frac{\int_0^{h_d} \Delta C(z) dz}{\Delta C_m} \quad (18)$$

to relate the global oceanic perturbation inventory to the surface ocean perturbation

$$\Delta N_{oc} = A_{oc} \int_0^{h_d} \Delta C(z) dz = A_{oc} H_{oc} \Delta C_m \quad (19)$$

If we assume that the surface DIC concentration perturbation has been increasing exponentially, that is, $\Delta C_m \sim e^{\mu t}$, then the time rate of change of the oceanic CO_2 inventory is related to the surface perturbation by

$$\dot{N}_{oc} = A_{oc} H_{oc} \mu \Delta C_m \quad (20)$$

The fourth relation is obtained from a similar equation formulated for the ^{13}C isotope, where we assume that the same penetration depth applies for physical mixing of ^{13}C as for total inorganic carbon:

$$\Delta^{13} N_{oc} = A_{oc} H_{oc} \Delta^{13} C_m \quad (21)$$

As in the case of CO_2, we assume an exponential perturbation in ^{13}C, that is, $\Delta^{13} C_m \sim e^{\mu t}$. We thus obtain for the rate of change of the oceanic ^{13}C inventory

$$^{13}\dot{N}_{oc} = A_{oc} H_{oc} \mu \Delta^{13} C_m \quad (22)$$

The marine biosphere complicates this approach in two ways. First the Suess effect of the oceanic organic carbon pool as discussed above in section 2.1 constitutes an additional reservoir of ^{13}C and would thus have to be included in the balance equation (17). Second, the marine biosphere also affects the redistribution of the ^{13}C isotope because marine organisms in the surface layer incorporate the ambient $^{13}C/^{12}C$ ratio into their tissue and calcareous shells. After their death some of the debris sink to depth and are remineralized to DIC. This constitutes an enhanced vertical transport and hence a larger penetration depth for ^{13}C as compared to CO_2. In the present context, both effects work in opposite directions and thus tend to cancel partially. Indeed, based on numerical calculations with reasonable values for the marine biospheric fluxes, we found that these affect the final solution only marginally and may thus be neglected.

We thus have postulated four basic relations: (16), (17), (20) and (22). Next, we reexpress the perturbation fluxes as functions of the perturbations in the atmosphere and surface oceans, respectively. Furthermore, total ^{13}C is replaced by the product of isotopic ratio and total carbon.

The perturbation fluxes of CO_2 may be reexpressed as functions of the atmospheric CO_2 partial pressure (ΔP_a) and of the surface DIC perturbation ΔC_m:

$$\Delta F_{am} = F_{am0} \frac{\Delta P_a}{P_{a0}} \quad (23)$$

$$\Delta F_{ma} = F_{ma0} \xi \frac{\Delta C_m}{C_{m0}} \quad (24)$$

where ξ denotes the buffer factor [*Broecker and Peng*, 1982]. The same is done for the perturbation fluxes of ^{13}C:

$$\begin{aligned} \Delta^{13} F_{am} &= \Delta(F_{am} \alpha_{am} R_a) \\ &= \alpha_{am}(R_a \Delta F_{am} + F_{am0} \Delta R_a) \\ &= \alpha_{am} F_{am0}((R_{a0} + \Delta R_a) \frac{\Delta P_a}{P_{a0}} + \Delta R_a) \end{aligned} \quad (25)$$

and

$$\begin{aligned} \Delta^{13} F_{ma} &= \Delta(F_{ma} \alpha_{ma} R_m) \\ &= \alpha_{ma}(R_m \Delta F_{ma} + F_{ma0} \Delta R_m) \\ &= \alpha_{ma} F_{ma0}((R_{m0} + \Delta R_m) \xi \frac{\Delta C_m}{C_{m0}} + \Delta R_m) \end{aligned} \quad (26)$$

$\Delta^{13} C_m$ can also be reexpressed in terms of ΔC_m and ΔR_m:

$$\Delta^{13} C_m = \Delta C_m (R_{m0} + \Delta R_m) + C_{m0} \Delta R_m \quad (27)$$

Using (6) the time rate change of the oceanic perturbation inventory in ^{13}C, $^{13}\dot{N}_{oc}$, is written as

$$^{13}\dot{N}_{oc} = \dot{N}_{oc} R_{oc} + A_{oc} C_{oc} \dot{D} \quad (28)$$

Assuming a steady state, the net preindustrial air-sea fluxes of total carbon and of ^{13}C must balance the land-ocean river transports by rivers:

$$F_{ma0} - F_{am0} = F_{r,org} + 0.5 F_{r,dic} \quad (29)$$

$$\begin{aligned} F_{ma0} \alpha_{ma} R_{m0} - F_{am} \alpha_{am} R_{a0} = \\ F_{r,org} R_{b0} + 0.5 F_{r,dic} R_{r,soil} \end{aligned} \quad (30)$$

However, numerical experimentation with reasonable values for the river fluxes [*Degens et al.*, 1991, *Sarmiento and Sundquist*, 1992] shows that these affect the final result only marginally and can be neglected.

All these auxillary expressions (23)-(30) can be inserted into the four basic equations (16), (17), (20), and (22). The four resulting equations are then reduced to a single relation by eliminating three unknowns: the product of the penetration depth times the exponential increase rate, $H_{oc}\mu$, and the perturbations of total carbon, ΔC_m, and of the isotopic ratio, ΔR_m, in the surface ocean layer. The resulting final equation relates the rate of change of the oceanic isotope ratio, $\dot{R}_{oc}$, to the oceanic CO_2 uptake rate, $\dot{N}_{oc}$.

The complete solution is given in Appendix A. After a few further approximations (see Appendix A) we obtain the final result:

$$A_{oc} C_{oc} \dot{D} = \dot{N}_{oc} \xi \frac{F_{am} \Delta R_a + R_{PDB}(\alpha_{ma} - 1) \dot{N}_{oc}}{F_{am} \frac{\Delta P_a}{P_{a0}} + \dot{N}_{oc}(\xi - 1 - 2 \frac{\Delta P_a}{P_{a0}})} \quad (31)$$

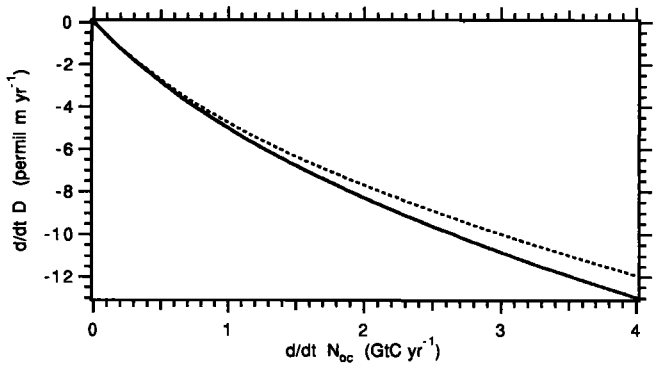

Figure 2. Time rate of change of the $^{13}C/^{12}C$ ratio of DIC (in permil meters per year) as a function of the oceanic CO_2 uptake rate (in gigatons carbon per year), calculated from equation (31). Parameter values are ξ=10.1, ΔR_a = -1.20 ‰, $\frac{\Delta P_a}{P_a}$ = 0.20, and $\alpha_{ma} - 1$ = -10.3 ‰. The two curves correspond to F_{am}=100 (solid line) and 80 GtC yr^{-1} (dashed line), respectively.

Equation (31) represents a weakly nonlinear relation between the time rate of change of the globally averaged oceanic $^{13}C/^{12}C$ isotope ratio, represented by $\dot{D}$, the vertically integrated time derivative of the oceanic isotope ratio (6), and the time rate of change in the oceanic carbon inventory, $\dot{N}_{oc}$. Given an estimate of $\dot{D}$, equation (31) may be numerically solved for $\dot{N}_{oc}$. The application of this equation requires the specification of numerical values for the gross air-sea flux of carbon, F_{am}, the buffer factor, ξ, the sea-air kinetic fractionation factor α_{ma}, and two quantities from the history of atmospheric carbon: the relative increase in atmospheric CO_2 concentration, $\frac{\Delta P_a}{P_{a0}}$, and the change in atmospheric $^{13}C/^{12}C$ ratio, $\Delta R_a = R_a - R_{a0}$, since preindustrial times. The relation is displayed graphically in Figure 2 for two different magnitudes of the air-sea exchange flux while the other parameter values are specified according to the consistent scenario (see the next section).

Despite the underlying assumptions and the approximations made in its derivation, equation (31) is rather robust. In order to explore its sensitivity with respect to the four assumptions listed in the introduction to this section, we performed several numerical simulation experiments with two different ocean carbon models, the one-dimensional box-diffusion model of *Oeschger et al.* [1975] and the three-dimensional HAMOCC 3 model (see section 3.1). Both models include a full description of the oceanic carbon chemistry and of the appropriate fractionation factors for the calculation of the ^{13}C carbon isotope. In each simulation experiment the ocean models were forced by the prescribed atmospheric CO_2 concentration and its $^{13}C/^{12}C$ ratio through the historical period 1800–1990.

In the base case we prescribed the atmospheric CO_2 concentration history by a smooth approximating spline curve fitted to the the data from ice cores [*Friedli et al.*, 1986] and the Mauna Loa record [*Keeling et al.*, 1989] as used in the recent Intergovernmental Panel on Climate Change (IPCC) global carbon cycle model intercomparison [*Enting et al.*, 1994]. The atmospheric $^{13}C/^{12}C$ ratio was specified in the base case as a stiff spline curve through the ice core data reported by *Friedli et al.* [1986] and the atmospheric observations of *Keeling et al.* [1989] (see Figure 3). Both models yield different ocean carbon uptake rates averaged over the time period 1970-

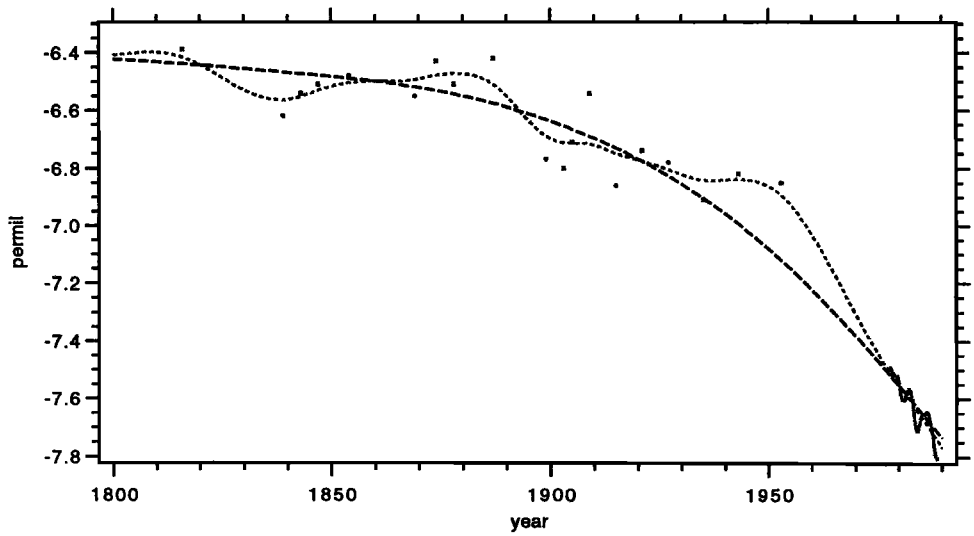

Figure 3. Atmospheric $^{13}C/^{12}C$ ratio specified in the numerical model simulations. Dashed line; base case and dotted line; loose spline used in the sensitivity calculation, see text. Ice core data (crosses) from *Friedli et al.*, [1986], direct atmospheric observations (solid line) from *Keeling et al.* [1989].

1990 (2.1 GtC yr^{-1} for the box-diffusion model and 1.3 GtC yr^{-1} for HAMOCC 3, see section 3.1) but also consistently different time derivatives of the isotope ratio of oceanic DIC (-8.6‰m yr^{-1} for the box-diffusion model and -5.7‰m yr^{-1} for HAMOCC 3). Applying formula (31) to these model results shows that it is correct to better than 5%.

In order to explore the sensitivity with respect to the assumption of an almost exponential increase of the atmospheric CO_2 concentration, we performed an additional numerical simulation with the box-diffusion model. Here we forced the model with an atmospheric CO_2 concentration history prescribed by a loose spline curve following closely the recent high-resolution icecore measurements reported by *Etheridge et al.* [1996], supplemented by the atmospheric CO_2 concentration data of *Keeling et al.* [1989; 1995]. This concentration record shows clear deviations from a pure exponentially rising trend, nevertheless, averaged over the time interval 1970-1990 equation (31) was found to be correct to better than 4%. As a further test, we also replaced the smooth atmospheric $^{13}C/^{12}C$ record with a loose spline curve through the icecore measurements of *Friedli et al.* [1986] (shown as dashed line in Figure 3). This again was found to have no noticeable effect on the validity of relation (31).

As a final sensitivity test, we explored two extreme future CO_2 concentration pathways over the time period 1990–2010. In each case, the box-diffusion model was forced as in the base case until 1990. Thereafter the atmospheric CO_2 concentration (1) was held constant at a level of 350 parts per million by volume (ppmv) (a very unlikely case as it could only be achieved with a drastic reduction in fossil emissions) or (2) was prescribed to increase linearly to 410 ppmv by the year 2010. The model calculated oceanic carbon uptake rates averaged over the 20 year time interval between 1990 and 2010 are computed as 2.0 GtC yr^{-1} in case (1) and 3.7 GtC yr^{-1} in case (2). Irrespective of the correspondingly prescribed change in atmospheric $^{13}C/^{12}C$ ratio relation (31) was found to be correct within 10%.

These sensitivity calculations demonstrate that the dynamical constraint as expressed in (31) is not critically dependent on the four assumptions stated in the introduction to this section. However, the dynamic constraint applies only to the passive ocean uptake capacity for excess atmospheric CO_2. Any air-sea flux of CO_2 driven by changes in the natural oceanic carbon cycle, such as during El Niño-Southern Oscillation (ENSO) events [*Winguth et al.*, 1994, *Keeling et al.*, 1995] can not be detected by the dynamical constraint. Hence (31) is only applicable over a time period sufficiently long as to exclude major contributions from changes in the natural oceanic carbon cycle, that is, over timescales of 10–20 years. This contrasts to the budget approaches proposed by QTW and TBK and must be kept in mind if the different methods are compared.

2.4. A Consistent Scenario

The application of the three methods developed in the previous sections requires the specification of numerical values for the carbon cycle parameters that enter the equations. Table 1 contains in the third column a list of a priori numerical values of the different global carbon cycle parameters. The data sources for these numerical values are described in Appendix B. The three last rows list the resulting ocean uptake rates calculated by each of the three methods (that is, using (8), (15), and (31)).

The chosen set of a priori values result in drastically different estimates for the ocean uptake rates: Using the method of QTW, we get 2.27 GtC yr^{-1}, by the method of TBK 0.64 GtC yr^{-1}, and based on the dynamic constraint 3.10 GtC yr^{-1}. The differences compared to the estimates given by QTW and TBK, respectively, result from the slightly different numerical values of the parameters chosen here, and, in the case of the TBK method, from the inclusion of the river transport term.

At first sight, the three approaches appear inconsistent. However, uncertainties in the carbon cycle input data must also be taken into account. We list in the third column of Table 1 for each of the parameters an assumed uncertainty, expressed as a standard deviation. Assuming that the uncertainty estimates of the a priori parameter values are not correlated, using the rules of error propagation we obtain considerable uncertainty estimates that have to be attributed to the ocean uptake rates calculated with the three formulas, ranging between 1.16 and 1.63 GtC yr^{-1}. In calculating the error of the dynamical constraint method we also include a potential formula error of 10%.

Several of the key parameters that might be responsible for the discrepancy between the results obtained with the atmosphere-ocean budget method as compared to the atmosphere budget method have been discussed by TBK. Here we adopt a different strategy in order to resolve this apparent paradox. Using an objective method, we attempt to construct a consistent scenario by simultaneously adjusting all parameters.

Formally, the problem may be stated as follows: (1) We are given a set of a priori parameter values, ω together with their uncertainties. (2) We are given a set of theoretical relations (that is, in our case (8), (15), and (31))

$$\mathbf{\Psi}(\mathbf{\Omega}) = 0 \tag{32}$$

and (3) we seek a set of a posteriori parameter values $\mathbf{\Omega}$, that fulfill the theoretical relations and at the same time, minimize the weighted distance to the a priori values:

$$S^2 = (\mathbf{\Omega} - \omega)^T \mathrm{C}_\omega (\mathbf{\Omega} - \omega) \tag{33}$$

Table 1. Global Carbon Cycle Parameters (Representative for 1970-1990)

Parameter (Units)	Symbol	A Priori Value[a]	A Priori σ[b]	A Posteriori Value[c]
Atmosphere				
Inventory (GtC)	N_a	715.	7.	715.0
Rate of change of inventory (GtC yr^{-1})	$\dot{N}_a$	3.0	0.3	2.94
Relative increase 1800–1980	$\frac{\Delta P_a}{P_{a0}}$	0.20	0.02	0.198
$^{13}C/^{12}C$ ratio (‰)	R_a	-7.55	0.10	-7.551
Rate of change of $^{13}C/^{12}C$ ratio (‰yr^{-1})	$\dot{R}_a$	-0.02	0.01	-0.023
Change in $^{13}C/^{12}C$ ratio 1800–1980 (‰)	ΔR_a	-1.10	0.15	-1.137
Fossil Fuel Source				
Fossil fuel CO_2 source (GtC yr^{-1})	Q_{foss}	5.1	0.3	5.09
$^{13}C/^{12}C$ ratio (‰)	R_{foss}	-28.1	0.5	-28.1
Terrestrial Biosphere				
Average $^{13}C/^{12}C$ ratio of biosphere to atmosphere CO_2 flux (‰)	R_b	-25.	2.0	-25.1
Terrestrial biospheric Suess effect (GtC ‰yr^{-1})	$F_{ab}(R_{ab}^{eq} - R_a)$	18.	12.	23.4
Ocean				
Air-sea gas exchange flux (GtC yr^{-1})	F_{am}	85.	21.	94.9
DIC concentration (mol C m^{-3})	$C_{oc} \approx C_m$	2.1	0.05	2.10
Buffer factor	ξ	10.5	1.0	10.59
$^{13}C/^{12}C$ ratio of DIC (‰)	$R_{oc} \approx R_m$	1.8	0.5	1.78
Kinetic air-sea fractionation factor (‰)	$\alpha_{ma} - 1$	-10.9	0.3	-10.91
Vertically integrated rate of change of $^{13}C/^{12}C$ in DIC (‰m yr^{-1})	$\dot{D}$	-10.4	3.0	-8.94
Air-sea isotopic disequilibrium (‰)	$R_{am}^{eq} - R_a$	0.43	0.20	0.533
Marine organic carbon Suess effect (GtC ‰yr^{-1})	$F_{ocb}(R_{mb}^{eq} - R_m)$	5.	5.	5.3
River Carbon Fluxes				
Inorganic carbon (GtC yr^{-1})	$F_{r,dic}$	0.4	0.3	0.40
Organic (dissolved and particulate) carbon transport (GtC yr^{-1})	$F_{r,org}$	0.4	0.3	0.44
Oceanic CO_2 Uptake (GtC yr^{-1})	$\dot{N}_{oc}$	2.	10.	2.12
Based on ocean-atmosphere ^{13}Cbudget (QTW)		2.27[d]	1.16[d]	
Based on atmosphere ^{13}C budget (TBK)		0.64[e]	1.59[e]	
Based on dynamic constraint		3.10[f]	1.63[f]	

[a]See Appendix B.
[b]One standard deviation, see Appendix B.
[c]Listed with one digit more than considered significant to indicate direction of change in optimization procedure.
[d]Based on equation (8)
[e]Based on equation (15)
[f]Based on equation (31)

where C_ω denotes the *a priori* covariance matrix of the parameters.

The technique to obtain the *a posteriori* values of the parameters (Ω) is called "total inversion" and is reviewed in a geophysical context by *Tarantola and Valette* [1982].

Applying this method to our problem we obtain a consistent scenario which is given by the set of a posteriori parameter values listed in the last column of Table 1. Thereby, the ocean uptake rate is assigned an a priori value of 2 GtC yr^{-1} with a very large (10 GtC yr^{-1}) uncertainty. The procedure yields an a posteriori "best" estimate for the ocean uptake of 2.1 GtC yr^{-1} with a standard deviation uncertainty of 0.9 GtC yr^{-1}.

Since we have only three relations and 20 adjustable parameters, the problem is underdetermined, and the a priori parameter values and their uncertainties crucially determine the solution. The largest adjustments are assigned (1) to the global air-sea isotopic disequilibrium, which increases from 0.43 to 0.53 ‰, (2) to the Suess effect of the terrestrial biosphere which is increased from 18 to 23 GtC‰yr^{-1}, (3) to the global air-sea gas exchange rate (increased from 85 to 95 GtC yr^{-1}) and (4) the rate of change of the $^{13}C/^{12}C$ ratio of oceanic DIC (increased from -10.4 to -8.9‰m yr^{-1}). However, none of the parameters is pushed by the minimization procedure outside of its assigned *a priori* standard deviation.

As discussed in Appendix B, we believe, that a global air-sea isotopic disequilibrium of 0.53 ‰ is not ruled out by the current observations and taking into account the uncertainties in the spatial distribution of the air-sea exchange coefficient. The Suess effect of the terrestrial biosphere is not directly observable and must be modelled, possibly cross checked by considering the penetration of bomb-^{14}C in soils [*Harrison et al.*, 1993]. A value of 23 GtC‰ yr^{-1} appears still acceptable and is still lower than the value calculated by *Enting et al.*, [1993] using a four-box compartment model described by *Emanuel et al.*, [1981]. The direction into which this parameter is pushed by the minimization procedure confirms the analysis performed by *Broecker and Peng* [1993].

2.5. Sensitivity Analysis

The three methods are finally compared by investigating the sensitivity of the estimated ocean CO_2 uptake rate with respect to uncertainties in the carbon cycle input data. Table 2 contains for each parameter its nominal value according to the consistent scenario and its assumed uncertainty (one standard deviation, σ). Assuming that these uncertainties are uncorrelated and using standard error propagation formulae, we can calculate the total variance that has to be attributed to the final result. Column 5 lists the contribution of the individual parameter to the total variance in the estimated oceanic uptake rate. Only input parameters that contribute more than 5% are listed. Columns 6

Table 2. Sensitivity Analysis of the Three Methods

Parameter[a]	Value	σ	Units	Varfraction %	Low GtC yr^{-1}	High GtC yr^{-1}
			Ocean-Atmosphere ^{13}C Budget (QTW)			
$\dot{D}$	-8.94	3.0	‰m yr^{-1}	73	3.11	1.14
$F_{ab}(R_{ab}^{eq} - R_a)$	23.4	12.	GtC ‰yr^{-1}	15	1.67	2.57
$\dot{R}_a$	-0.023	0.010	‰yr^{-1}	5	2.39	1.86
$\dot{N}_{oc}$	2.12	1.15	GtC yr^{-1}	100	0.97	3.27
			Atmosphere ^{13}C Budget (TBK)			
$R_{am}^{eq} - R_a$	0.53	0.20	‰	48	0.93	3.31
$F_{ab}(R_{ab}^{eq} - R_a)$	23.4	12.	GtC ‰yr^{-1}	19	1.37	2.87
F_{am}	94.9	21.	GtC yr^{-1}	17	1.42	2.82
$\dot{R}_a$	-0.023	0.01	‰yr^{-1}	7	2.57	1.67
$\dot{N}_{oc}$	2.12	1.71	GtC yr^{-1}	100	0.41	3.83
			Dynamic Constraint			
$\dot{D}$	-8.94	3.0	‰m yr^{-1}	78	3.32	1.19
ΔR_a	-1.14	0.15	‰	8	1.81	2.51
ϵ[b]	0.	0.1		7	1.81	2.51
$\dot{N}_{oc}$	2.12	1.21	GtC yr^{-1}	100	0.91	3.33

[a]Only variables shown that contribute more than 5% to the global variance estimate

[b]Relative error of equation (31)

and 7 report the range of ocean uptake estimates that is spanned if only the parameter listed in the corresponding row is varied from one standard deviation below ("Low") to one standard deviation above ("High") its nominal value.

Table 2 clearly reveals the most crucial parameters of each method:

1. The error in the ocean uptake estimate based on the ocean-atmosphere method is determined primarily by the uncertainty in the time derivative of the oceanic isotope ratio. But 27% of the total error variance are contributed by uncertainties of the terrestrial biospheric Suess effect, the fossil fuel $^{13}C/^{12}C$ ratio and the rate of change of the atmospheric $^{13}C/^{12}C$ ratio. These increase the total error estimate to 1.15 GtC yr^{-1}, larger than the error reported by QTW, which assumed smaller errors in these other terms.

2. The error in the ocean uptake estimate based on the atmosphere budget method is dominated by the uncertainty of the isotopic air-sea disequilibrium. However, here the uncertainties of the other terms in the balance equation contribute over 50% to the total error estimate of 1.71 GtC yr^{-1}.

3. In the case of the dynamic constraint method the uncertainty in $\dot{D}$ dominates with 78% the total error variance. A possible formula error of (31) of 10% contributes only 7% to the total uncertainty of 1.21 GtC yr^{-1}.

The result that the error estimates of each method applied separately are larger than the error estimate obtained in the minimization procedure indicates that none of the three relations is redundant. But the information content of the three equations is not equal as witnessed by the different uncertainty estimates.

Finally, we illustrate the sensitivities of the three methods by assuming hypothetically that the uncertainty of two key quantities, the oceanic $^{13}C/^{12}C$ ratio change, $\dot{D}$, and the air-sea isotopic disequilibrium, $R_{am}^{eq} - R_a$, were reduced by a factor of 2 due to, for example, extended observational programs. Such an improved knowledge of these quantities probably might represent the achievable maximum within the next decade. Because of the uncertainties in the other parameters, the error of the ocean uptake estimate is not reduced by a factor of 2 but only by 32% in the case of the ocean-atmosphere ^{13}C budget method (to 0.78 GtC yr^{-1}), by 20% in the case of the atmosphere ^{13}C budget method (to 1.36 GtC yr^{-1}), and by 36% in the case of the dynamic constraint method (to 0.78 GtC yr^{-1}).

On the basis of these considerations the dynamic constraint and the ocean-atmosphere ^{13}C budget method of QTW appear to yield smaller errors, especially in view of extended observational programs to come. However, the present comparison is strictly limited to the sensitivities of the different methods with respect to uncertainties in the available carbon cycle data. If the overall relative merits of the three approaches were to be judged, then other factors would also have to be taken into account, such as, for example, needed sampling strategy in space and time in order to determine the critical oceanic $^{13}C/^{12}C$ ratio properties.

On the other hand, the foregoing calculations also show the accuracy limits of the ^{13}C isotope method to determine the oceanic CO_2 uptake. Clearly, even extended observational programs will not push the error (one standard deviation) to below 0.5 GtC yr^{-1}.

3. Three-Dimensional Ocean Carbon Cycle Model Simulations

In order to illustrate the relationship between the oceanic penetration of CO_2, ^{13}C, and radiocarbon, two simulation experiments by means of the three-dimensional Hamburg model of the oceanic carbon cycle (HAMOCC 3) have been performed. Earlier versions of the Hamburg model of the oceanic carbon cycle have been reported by *Maier-Reimer and Hasselmann* [1987], *Maier-Reimer and Bacastow* [1990], and *Bacastow and Maier-Reimer* [1990]. A detailed description of the model in its present form is given by *Maier-Reimer* [1993].

The ocean carbon cycle model is embedded in the three-dimensional flow field calculated by the "large-scale geostrophic" ocean circulation model [*Maier-Reimer et al.*, 1993]. The model includes as primary variables dissolved inorganic carbon (DIC), PO_4, Si, Alkalinity, and O_2. On the basis of available light, nutrients, and vertical mixing the model computes the formation of organic material and calcareous shells by the marine biosphere and it portrays their sinking, remineralization at depth and burial in sediments. For diagnostic purposes in addition to bulk carbon, also the isotopic forms of ^{13}C and ^{14}C are kept track of. The current spatial resolution of the model is approximately 3.5° by 3.5° with 15 layers in the vertical dimension. With a time step of 1 month the model resolves, albeit crudely, the seasonal cycle.

3.1. Specifications of the Simulation Experiments

The two model simulation experiments discussed here differ in their gas exchange formulation at the surface: model run K employed a spatially and temporally constant gas exchange coefficient, set at a value of 0.06 molC m^{-2} yr^{-1} μatm^{-1}. In the model run V, a variable coefficient depending on wind speed and sea surface temperature according to the parametriza-

tion by *Liss and Merlivat* [1986] was prescribed. This parametrization was evaluated using global fields of monthly mean wind speed and standard deviation determined from meteorological analyses of the European Center for Medium Range Weather Forecast (ECMWF) and from the Comprehensive Ocean-Atmosphere Data Set (COADS) data set [*Woodruff et al.* 1987]. Details of this calculation are described by *Heimann and Monfray* [1989]. It is known that the parameterization by *Liss and Merlivat* [1986] together with realistic surface wind speeds leads to a globally averaged gas exchange coefficient for CO_2 which is almost 30% smaller than the value inferred from studies of the oceanic uptake of bomb radiocarbon [*Broecker et al.*, 1985, 1995]. The reasons for this discrepancy are not clear [*Watson*, 1993, *Wanninkhof*, 1992, *Hesshaimer et al.*, 1994]. Here we scaled the coefficients determined by the Liss and Merlivat formula by a factor of approximately 1.7 to obtain the same global average as in model run K.

In the model simulations described here, the model was firstly run to equilibrium (3000 simulated years). The resulting state was assumed to represent preindustrial conditions. Subsequently, the model was run through the time period 1750–1988 by prescribing the time evolution of the globally averaged atmospheric CO_2 concentration and its $^{13}C/^{12}C$ and $^{14}C/C$ isotopic ratios.

The atmospheric CO_2 concentration and its $^{13}C/^{12}C$ isotope ratio time history employed in the simulation has been described in the previous section. The atmospheric ^{14}C isotopic composition was prescribed in three latitude bands (north of 30°N, 30°S-30°N, south of 30°S), based on a combination of the data reported by *Stuiver and Quay* [1981] for the prebomb period and by *Nydal* [1983] and *Broecker and Peng* [1993] for the period after 1950.

The model predicted fields for 1973 are assumed to represent the time of the Geochemical Ocean Sections Study (GEOSECS). All reported time rates of change were determined from the difference between 1988 and 1973; hence represent time averages over 15 years centered approximately around 1980. Table 3 summarizes globally averaged key properties of the two model runs.

The global CO_2 uptake of the model, 1.29 (run K), respectively 1.33 $GtCyr^{-1}$ (run V) is smaller than calculated by other simpler box models or other ocean general circulation model (OGCM) based ocean carbon models [*Siegenthaler and Sarmiento*, 1993; *Sarmiento et al.*, 1992; *Schimel et al.*, 1995], which may be attributed to a generally too shallow predicted thermocline in the version of HAMOCC 3 used in the present study. Consistently, the model also predicts a much smaller globally averaged oceanic rate of change of the $^{13}C/^{12}C$ ratio of -5.6 (run K), and -5.8‰ m yr^{-1} (run V) as compared to the observations of -10‰ m yr^{-1} [QTW]. The predicted oceanic bomb ^{14}C inventories and the surface water bomb ^{14}C concentrations are larger than direct estimates from the observations [*Broecker et al.*, 1985, 1995], indicating that the specified globally averaged value of the gas exchange coefficient of 0.06 molC m^{-2} yr^{-1} μatm^{-1} appears to be about 10% too large. The global penetration depths of the ^{14}C penetration is less than 8% smaller than the observations. However, these model deficiencies, while quantitatively significant, are not expected to invalidate the main purpose of the present analysis, that is, the intercomparison of the dynamical behavior of the different carbon tracers.

3.2. The Relationship Between the Rate of Change of Excess Dissolved Inorganic Carbon, $^{13}C/^{12}C$ Ratio and the Inventory of Bomb ^{14}C

Here we focus on the relations between the three different carbon tracers for which the HAMOCC 3 simulations provide a convenient illustration. In particular, we investigate the penetration of (1) excess dissolved

Table 3. Global Properties of OCCM Simulation Runs

Variable	Run K	Run V	Observations	Units
Oceanic CO_2 uptake (average 1973–1988)	1.29	1.33		GtC yr^{-1}
Oceanic $^{13}C/^{12}C$ ratio rate of change	-5.60	-5.76	-10.4[a]	‰m yr^{-1}
Surface $^{13}C/^{12}C$ ratio rate of change	-0.0135	-0.0134	-0.02[a]	‰yr^{-1}
Bomb ^{14}C inventory (1973)	9.38	9.27	8.4[b]	10^9 at ^{14}C cm^{-2}
Change in surface ^{14}C concentration 1950–1973	206	189	157[b]	‰

[a][*Quay et al.*, 1992]
[b][*Broecker et al.* 1985]

inorganic carbon as described by the rate of change of the vertically integrated carbon inventory $\dot{I}$ (expressed in mol carbon per square meter per year), (2) ^{13}C, described by the vertically integrated rate of change of the $^{13}C/^{12}C$ ratio (expressed in permil meters per year, see equation (7)), and (3) bomb radiocarbon as described by the inventory of bomb ^{14}C approximately at the time of GEOSECS (1973, expressed in atoms ^{14}Cper square meter).

Figures 4a–4c and 5a–5c show the global geographic pattern of the three quantities computed in the two model runs.

The combination of three general factors determines the penetration of the three transient tracers: gas exchange, atmospheric forcing history, and transport to depth within the ocean (primarily into the thermocline). As demonstrated before [e.g. *Sarmiento et al.*, 1992], the the uptake of anthropogenic CO_2 is primarily controlled by internal transport within the upper ocean. On the other hand, both ^{13}C and bomb ^{14}C are also limited to a considerable amount by the gas exchange process at the surface. However, the atmospheric forcing history of the two isotopic tracers is quite different, ^{13}C showing an exponential perturbation with a time constant of approximately 30 years similar to CO_2, whereas the history of atmospheric bomb ^{14}C shows a pronounced peak in the early 1960s followed by a decline in the following 10 years up to the GEOSECS program [*Broecker and Peng*, 1993]. On the basis of this, we expect the behavior of the spatial pattern of the ^{13}C perturbation to lie intermediate between DIC and bomb ^{14}C.

Evidently, the fields of excess DIC and ^{13}C exhibit very similar spatial structures (see Figures 4a, 4b and 5a, 5b), demonstrating, that the oceanic $^{13}C/^{12}C$ perturbation appears to track, at least qualitatively, the penetration of anthropogenic carbon. Largest rates of change are seen in the North Atlantic where newly formed North Atlantic Deep Water carries the perturbation to depth. Relative maxima also occur in the western parts of the subtropical gyres in all major oceans. Here the pattern reflects the vertical extent of the upper thermocline where both transient tracers are accumulating.

On the other hand, bomb-^{14}C does not perfectly track anthropogenic CO_2 in the ocean. Figures 4c and 5c show the horizontal distribution of the bomb-^{14}C inventory as predicted by the two model simulations. While there is an overall similarity to the patterns exhibited by the two other tracers (Atlantic versus Pacific and Indian Ocean, subtropical gyre maxima versus lower values in the equatorial region), there nevertheless exist significant differences. Most conspicuously in model run V, the maxima in the subtropical gyres are located in the eastern part of the ocean basins (except in the North Atlantic) in the areas of intense recirculation and most strongly depressed thermocline [*Toggweiler et al.*, 1989]. In contrast, total carbon and the $^{13}C/^{12}C$ ratio are accumulating predominantly in the western part of the subtropical gyres. This demonstrates the different input history of the tracers: Bomb-^{14}C is entering the sea predominantly in latitudes poleward of the subtropical gyres where, at least in model run V, gas exchange rates are higher. In the 10 years following the peak input, the bomb ^{14}C had time only to spread around the subtropical gyres toward the east. In contrast, the more uniform penetration of ^{13}C and of total carbon on a longer timescale allow for a more homogenous distribution within the upper thermocline.

The direct relation between the perturbations of ^{13}C and of DIC is demonstrated in Figures 6a and 6b in the form of a scatterplot. In these plots each point corresponds to a vertical integral calculated at a horizontal grid point of the OCCM. If the model ocean were a pure collection of parallel, one-dimensional vertical columns, each with identical surface temperature and gas exchange coefficient, then all points would lie on the same theoretical relationship (31) derived in the previous section. Evidently, the three-dimensional ocean circulation is not as simple, hence the scatter of the points.

The scatterplots show that the two tracers correlate (r^2=0.96 in both model runs), but not perfectly. These plots demonstrate indeed, that the local oceanic carbon inventory change may be estimated by monitoring the $^{13}C/^{12}C$ isotope ratio change. Given an observation of $\dot{D}$ at a particular location, an estimate of $\dot{I}$ can be made with an uncertainty smaller than 50% based on the spread of the datapoints.

In contrast, Figures 7a and 7b summarize in the form of a scatterplot the relation between the bomb-^{14}C inventory and the rate of change DIC. The large scatter of the points illustrates that a direct local estimate of the oceans excess carbon storage from bomb-^{14}C data alone is not possible.

3.3. The Relation Between the Air-Sea Input Flux and the Induced Inventory Changes

Finally, we address the relation between the oceanic input functions, that is, the air-sea tracer fluxes and the induced inventory changes of the three carbon tracers. Figure 8a shows for the model run V the zonally averaged inventory change in DIC (dashed line). The distribution is fairly uniform with latitude with a slight enhancement in the subtropical gyres. This inventory change is caused by a surface perturbation "forcing" S, which we define as

$$S = \Delta(\phi_{am} - \phi_{ma}) \tag{34}$$

where ϕ_{am} and ϕ_{ma} denote the air-sea, respectively sea-

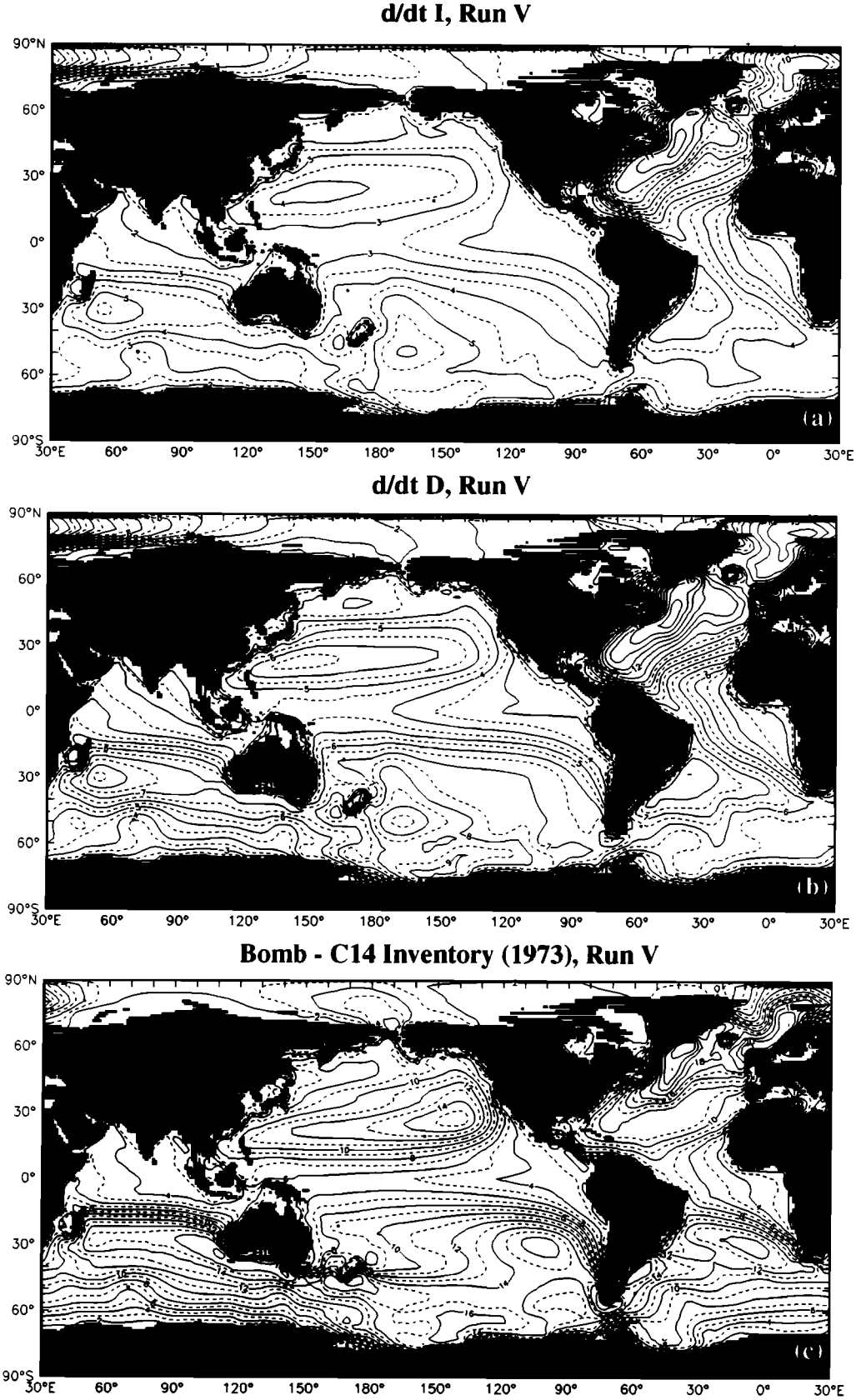

Figure 4. (a) Vertically integrated rate of change in carbon inventory, average 1973–1988 (in moles carbon per square meters per year), (b) Vertically integrated rate of change in $^{13}C/^{12}C$ isotope ratio, average 1973–1988 (in permil meters per year), (c) Inventory of bomb produced radiocarbon in 1973, (in 10^9 atoms per square centimeters). Model run V (variable gas exchange coefficient).

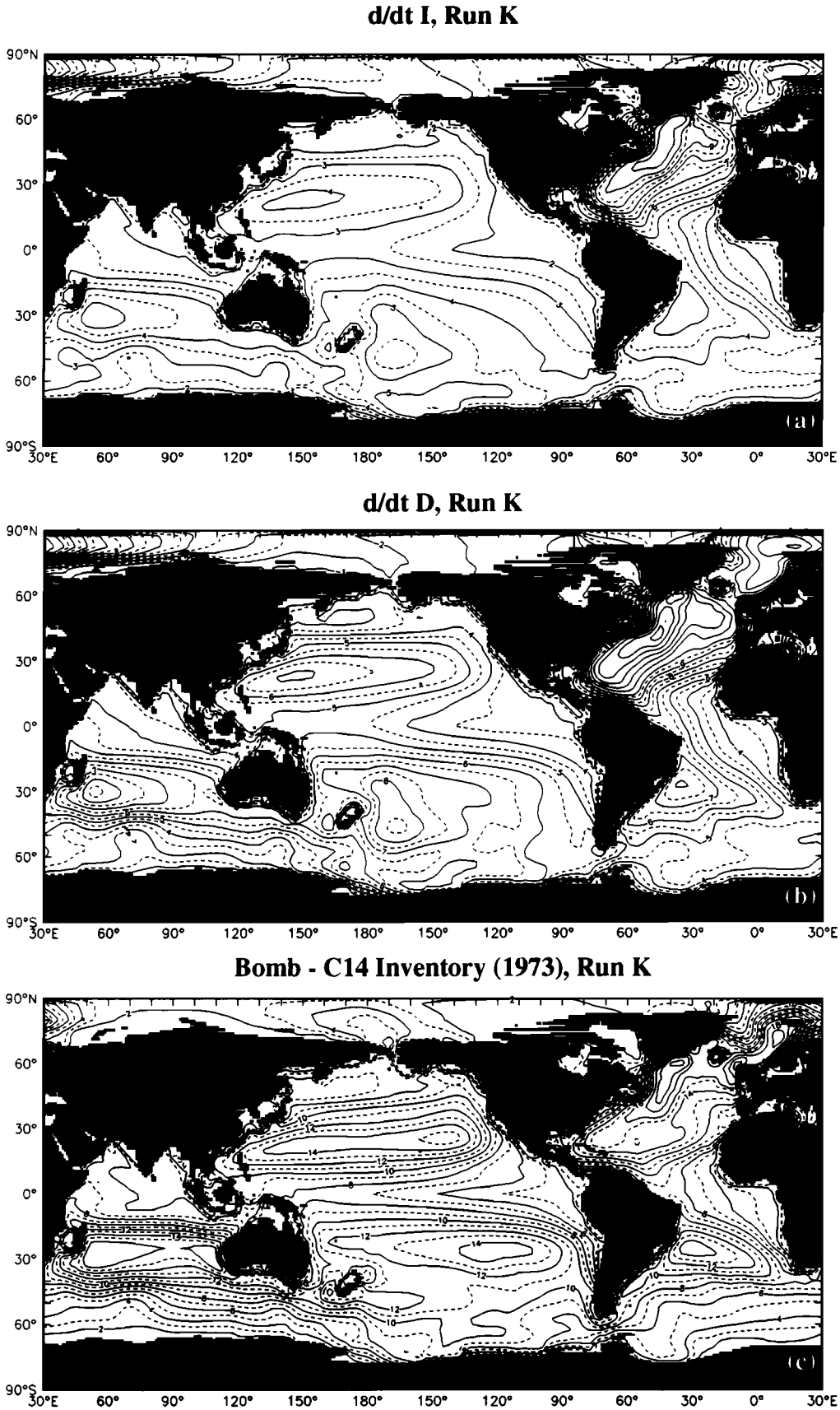

Figure 5. Same as Figure 4 but for model run K (constant gas exchange coefficient).

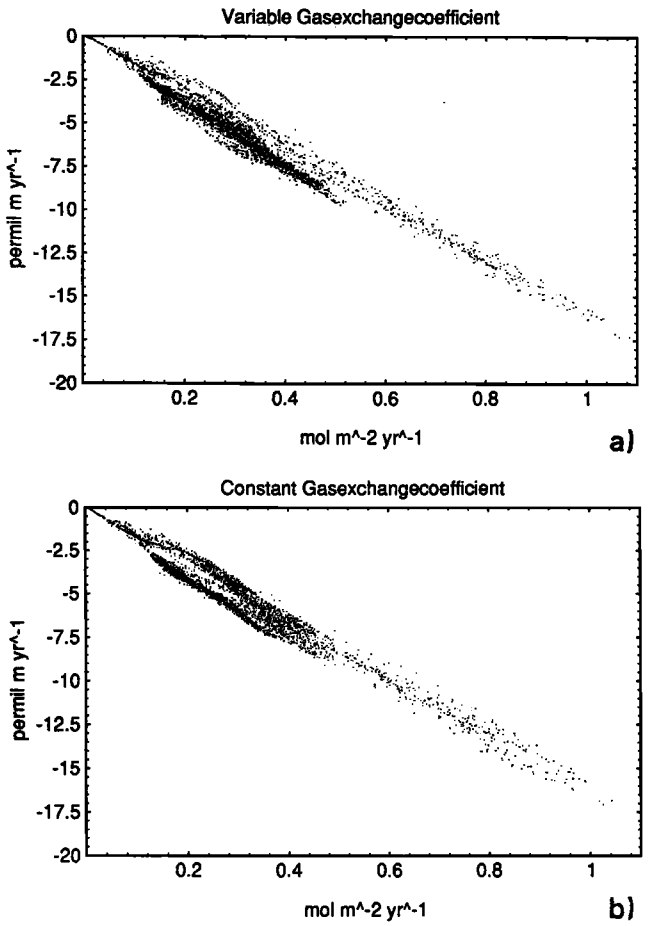

Figure 6. Vertically integrated rate of change in $^{13}C/^{12}C$ isotope ratio, $\dot{D}$, versus vertically integrated rate of change in carbon inventory per unit area: (a) model run V (variable gas exchange coefficient), (b) model run K (constant gas exchange coefficient).

air CO_2 fluxes (expressed in gC m^{-2} yr^{-1}). Δ indicates the difference with respect to preindustrial values (see equation 16). This perturbation air-sea flux of carbon, zonally averaged, is also shown in Figure 8a (solid line). The latitudinal distribution of this perturbation influx is dominated by regions where surface waters are in close contact with deeper and older waters, that is, in high latitudes and close to the equator. The local minimum directly at the equator reflects the very small gas exchange rates in this location.

Figure 8b shows a similar plot but for the ^{13}C isotope. The dashed line represents the zonally averaged, vertically integrated rate of change of the ^{13}C ratio, $\dot{D}$. In analogy to the perturbation forcing of total carbon, we have to define an "air-sea isotopic ratio forcing". The ^{13}C rate of change a water parcel experiences when it comes in contact with the atmosphere is given by

$$\frac{d}{dt}R_m C_m = \Delta(^{13}\phi_{am} - {}^{13}\phi_{ma}) \tag{35}$$

hence the rate of $^{13}C/^{12}C$ ratio change is

$$\begin{aligned} C_m \frac{d}{dt} R_m & \\ &= \Delta(^{13}\phi_{am} - {}^{13}\phi_{ma}) - R_m \frac{d}{dt} C_m \\ &= \Delta(^{13}\phi_{am} - {}^{13}\phi_{ma}) - R_m \Delta(\phi_{am} - \phi_{ma}) \end{aligned} \tag{36}$$

hence the isotopic ratio forcing, ^{13}S, can be defined as

$$^{13}S = \frac{\Delta(^{13}\phi_{am} - {}^{13}\phi_{ma})}{R_m C_m} - \frac{\Delta(\phi_{am} - \phi_{ma})}{C_m} \tag{37}$$

In analogy to the derivation of equation 13 we can approximate this as

$$^{13}S \approx \frac{\phi_{am}\alpha_{am}(\Delta R_a - \Delta R_m)}{C_m R_m} + \frac{S(\alpha_{ma} - 1)}{C_m} \tag{38}$$

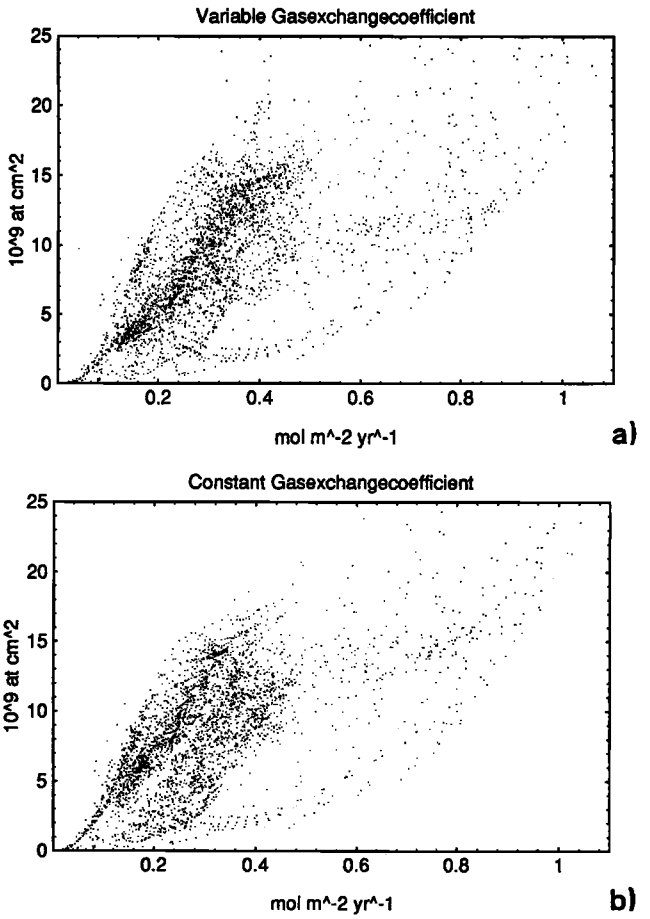

Figure 7. Bomb radiocarbon inventory versus vertically integrated rate of change in carbon inventory per unit area: (a) model run V (variable gas exchange coefficient), (b) model run K (constant gas exchange coefficient).

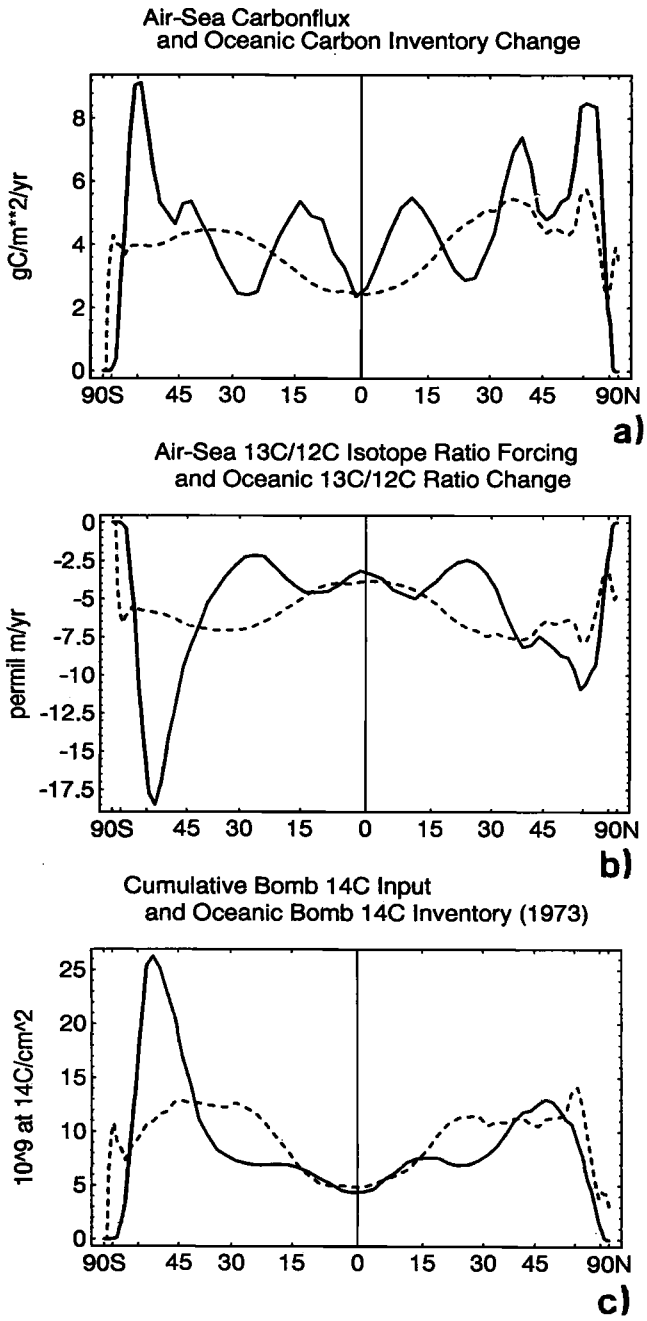

Figure 8. Zonally averaged perturbation inputs (solid lines) and inventories, respectively rates of inventory change (dashed lines) of the three transient tracers, all expressed per unit of ocean area: (a) total carbon, (b) $^{13}C/^{12}C$ ratio, (c) bomb radiocarbon.

It is straightforward to show that the isotopic ratio forcing, ^{13}S thus defined has the same units as $\dot{D}$ and that the global integrals of both quantities are equal. The zonal average of ^{13}S is also plotted in Figure 8b as a function of latitude (solid line). Finally, Figure 8c shows the zonally averaged bomb radiocarbon inventory (dashed line) and the zonally averaged integral of the air-sea flux of bomb radiocarbon (solid line).

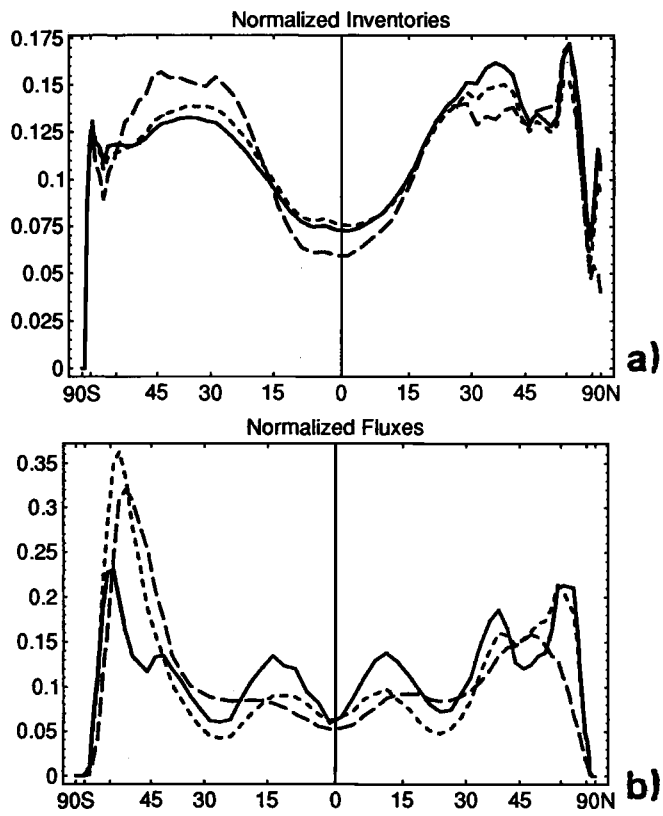

Figure 9. (a) Zonally averaged normalized inventory, respectively rates of inventory change of the three transient tracers: total carbon (solid line), $^{13}C/^{12}C$ ratio (short dashes) and bomb radiocarbon (long dashes). (b) Zonally averaged normalized perturbation input forcings: total carbon (solid line), $^{13}C/^{12}C$ ratio (short dashes) and bomb radiocarbon (long dashes).

The differences between the three transient tracers are more easily seen after a normalization. In Figure 9a the three inventory curves are normalized to the same global integral. The remarkable similarity between the $^{13}C/^{12}C$ ratio (short dashes) and the total carbon perturbation (solid line) is evident. In contrast, the bomb radiocarbon inventory is more displaced poleward.

Figure 9b shows the three input curves normalized to the same global integral. Here clear differences are apparent which reflect the different dynamics of the air-sea transfer of the three tracers. *Sarmiento et al.* [1992] noted the large differences between the input functions of bomb ^{14}C and anthropogenic CO_2, in particular, in the southern ocean in regions of high gas exchange rates. The $^{13}C/^{12}C$ ratio perturbation also shows this behavior, but in the remainder of the ocean ^{13}C follows more closely the anthropogenic CO_2 input than to the bomb ^{14}C.

4. Conclusions

On the basis of the present investigation we draw the following main conclusions:

1. The global analysis demonstrates, that the change of the $^{13}C/^{12}C$ ratio in the ocean can be translated into an approximate oceanic CO_2 uptake rate in an essentially model independent way.
2. The apparent discrepancies between the ocean uptake rates inferred with the analysis methods as developed by *Quay et al.*, [1992], *Tans et al.*, [1993], or based on the dynamic constraint might simply reflect uncertainties in the present observational database and do not require major revisions of our understanding of the global carbon cycle.
3. The three-dimensional ocean carbon cycle model simulations illustrate that the oceanic penetration of the $^{13}C/^{12}C$ signal may serve to a considerable extent as an analogue tracer of the oceanic perturbation with excess anthropogenic carbon.
4. In comparison, bomb ^{14}C, because of its different dynamics and atmospheric forcing history, constitutes a much less useful tracer to directly track the excess anthropogenic CO_2 in the ocean.

We emphasize, however, that the last point mentioned above does not imply that the information from bomb ^{14}C is useless. It is less useful as an analogue tracer of anthropogenic CO_2, but it nevertheless represents a key validation test for ocean models [*Toggweiler et al.*, 1989; *Sarmiento et al.*, 1992], in particular, also because of the existing extensive global database [*Broecker et al.*, 1985, 1995].

On the other hand, the present results demonstrate, that an extension of the oceanic ^{13}C database should receive a relatively high priority in future observational programs. It is clear, however, that the errors in the estimates of the oceanic CO_2 uptake rate can only be narrowed by means of a multitude of approaches. The ^{13}C method should be one of them.

Appendix A: Derivation of Equation (31)

The four basic relations (16), (17), (20), and (22) developed in section 2 are rewritten here after replacing the perturbation fluxes by the expressions (23)-(28):

$$\dot{N}_{oc} = F_{am0}\frac{\Delta P_a}{P_{a0}} - F_{ma0}\xi\frac{\Delta C_m}{C_{m0}} \tag{A1}$$

$$\dot{N}_{oc}R_{oc} + A_{oc}C_{oc}\dot{D} = \alpha_{am}F_{am0}\left((R_{a0}+\Delta R_a)\frac{\Delta P_a}{P_{a0}} + \Delta R_a\right) - \alpha_{ma}F_{ma0}\left((R_{m0}+\Delta R_m)\xi\frac{\Delta C_m}{C_{m0}} + \Delta R_m\right) \tag{A2}$$

$$\dot{N}_{oc} = A_{oc}H_{oc}\mu\Delta C_m \tag{A3}$$

$$\dot{N}_{oc}R_{oc} + A_{oc}C_{oc}\dot{D} = A_{oc}H_{oc}\mu\left[\Delta C_m(R_{m0}+\Delta R_m) + C_{m0}\Delta R_m\right] \tag{A4}$$

We approximate R_{oc} by R_{m0} and C_{oc} by C_{m0}. Furthermore, ignoring the river fluxes equations (29) and (30) imply $F_{ma0} \approx F_{am0}$ and $\alpha_{ma}R_{m0} \approx \alpha_{am}R_{a0}$. Using the notation

$$\phi_0 = F_{am0} \tag{A5}$$

$$\gamma = C_{m0}A_{oc}H_{oc}\mu \tag{A6}$$

$$d = \frac{A_{oc}C_{oc}\dot{D}}{R_{m0}} \tag{A7}$$

$$\nu_a = \frac{\Delta P_a}{P_{a0}} \tag{A8}$$

$$\nu_m = \frac{\Delta C_m}{C_{m0}} \tag{A9}$$

$$\rho_a = \frac{\Delta R_a}{R_{a0}} \tag{A10}$$

$$\rho_m = \frac{\Delta R_m}{R_{m0}} \tag{A11}$$

the four equations can be rewritten in simplified form as

$$\dot{N}_{oc} = \phi_0(\nu_a - \xi\nu_m) \tag{A12}$$

$$\dot{N}_{oc} + d = \alpha_{ma}\phi_0\left[\nu_a(1+\rho_a) + \rho_a - \xi\nu_m(1+\rho_m) - \rho_m\right] \tag{A13}$$

$$\dot{N}_{oc} = \gamma\nu_m \tag{A14}$$

$$\dot{N}_{oc} + d = \gamma(\nu_m + \rho_m) \tag{A15}$$

In forming the last equation, we have ignored the small product of $\nu_m\rho_m$ of perturbation terms.

These four equations are reduced to a single relation by eliminating the variables ν_m, ρ_m, and γ. After solving for d we obtain

$$d = \dot{N}_{oc}\xi\left[\alpha_{ma}\phi_0\rho_a(1+\nu_a) + \dot{N}_{oc}(\alpha_{ma}-1)\right]\left[\alpha_{ma}\frac{\dot{N}_{oc}^2}{\phi_0} + \alpha_{ma}\nu_a\phi_0(1+\nu_a) + \dot{N}_{oc}(\xi - \alpha_{ma}(1+2\nu_a))\right]^{-1} \tag{A16}$$

The preindustrial gross air-sea gas exchange flux, ϕ_0, is on the order of 80 GtC yr^{-1}, thus at least an order of magnitude larger than the current oceanic CO_2 uptake rate. Therefore the first term in the denominator of equation (A16) is small compared to the two other terms and can be neglected. Furthermore, the fractionation factor α_{ma} can be replaced by unity except in the second term in the numerator. The simplified formula then results in

$$d = \dot{N}_{oc}\xi\frac{\phi_0\rho_a(1+\nu_a)+\dot{N}_{oc}(\alpha_{ma}-1)}{\nu_a\phi_0(1+\nu_a)+\dot{N}_{oc}(\xi-1-2\nu_a)} \quad \text{(A17)}$$

which, after back substitution of the abbreviations (A5)-(A11) gives

$$\frac{A_{oc}C_{oc}\dot{D}}{R_{m0}} = \dot{N}_{oc}\xi\frac{\frac{F_{am}\Delta R_a}{R_{a0}}+(\alpha_{ma}-1)\dot{N}_{oc}}{F_{am}\frac{\Delta P_a}{P_{a0}}+\dot{N}_{oc}(\xi-1-2\frac{\Delta P_a}{P_{a0}})} \quad \text{(A18)}$$

As a final approximation we replace R_{m0} and R_{a0} by the standard isotopic ratio R_{PDB}. After rearrangement, this results in equation (31) given in section 2.3.

Appendix B: A Priori Global Carbon Cycle Parameter Values and Uncertainty Ranges

This appendix contains references and further comments on the adopted a priori values and uncertainty ranges (expressed as one standard deviation) in Table 1. All parameter values, unless stated otherwise, refer to the 20-year average 1970–1989.

Atmosphere

The atmospheric carbon inventory of 715 GtC [TBK] corresponds to a globally averaged CO_2 mixing ratio (average 1970–1989) of 337 ppmv. This value is assigned an uncertainty of 3 ppmv. The average rate of change of the atmospheric CO_2 mixing ratio over this period is 1.40 ppmv yr^{-1} based on the average of the Mauna Loa and the South Pole records [*Keeling et al.*, 1989; *Keeling et al.*, 1995]. This increase rate is assigned an uncertainty of 3 ppmv in 20 years or 10%. The 20% relative increase of the atmospheric mixing ratio since 1980 is calculated based on a preindustrial mixing ratio of 280 ppmv [*Friedli et al.*, 1986; *Leuenberger et al.*, 1992]. Preindustrial fluctuations in atmospheric CO_2 were on the order of less than 10 ppmv [*Barnola et al.*, 1995], an uncertainty of about 10% of the observed increase of 60 ppmv (1800–1980).

We use an average atmospheric $^{13}C/^{12}C$ ratio of -7.55‰ based on the average of the Mauna Loa and South Pole records [*Keeling et al.*, 1989], averaged over 4 years centered on January 1980, and assign it an error estimate of ±0.1‰. The atmospheric $^{13}C/^{12}C$ ratio has been monitored directly since 1978 [*Keeling et al.*, 1989] while the ice core record of *Friedli et al.* [1986] extends only through 1956. Thus for the time period 1970–1978 extrapolation or interpolation methods are required. QTB extrapolated the atmospheric record back in time based on the correlation with atmospheric CO_2 and quote an average (1970–1990) rate of change of the atmospheric $^{13}C/^{12}C$ ratio of -0.020‰ yr^{-1} based on an extrapolated value of -7.36‰ in 1970. This rate of change is rather uncertain: for example, a linear interpolation between the last ice core data point of *Friedli et al.*, [1986] and the beginning of the atmospheric record in 1978 would yield a value of -7.26 in 1970. Furthermore, the Scripps-Groningen atmospheric $^{13}C/^{12}C$ ratio record exhibits substantial fluctuations on the ENSO timescale which make an accurate long-term trend determination difficult. On the basis of these considerations we assign an uncertainty of ±0.01‰ yr^{-1} to the rate of change of the atmospheric $^{13}C/^{12}C$ ratio.

The preindustrial (~1800) atmospheric ^{13}C level has been determined by *Leuenberger et al.* [1992]: -6.45‰, yielding an isotopic shift 1800–1980 of -1.10‰. These authors quote uncertainty estimates of ±0.12‰ representing two standard deviations of the statistical error of the measurements. Potential systematic errors also have to be taken into account since several corrections have to be applied to the data which are difficult to quantify [*Leuenberger et al.*, 1992]. Considering also the uncertainty in the present atmospheric $^{13}C/^{12}C$ ratio, we assign the shift 1800–1980 an uncertainty estimate of ±0.15‰.

Fossil Fuel CO_2 Source

Fossil fuel CO_2 emissions 1970–1989 averaged 5.1 GtC yr^{-1} [*Marland and Boden*, 1993]. *Marland and Rotty* [1984] attribute an uncertainty of 10% (at the 90% confidence level) to their method, which implies a one standard deviation uncertainty of ±0.3 GtC yr^{-1} of the fossil fuel emission estimate.

The $^{13}C/^{12}C$ ratio of fossil fuel CO_2 has recently been redetermined [*Andres et al.*, 1996], giving -28.1‰ as an average 1970–1989. This value is attributed an uncertainty estimate of ±0.5‰.

Terrestrial Biosphere

The averaged $^{13}C/^{12}C$ ratio of CO_2 released by the current terrestrial biosphere is rather uncertain, however, its absolute value does not constitute a critical parameter in the present analysis. We set it to -25‰ and assign it an uncertainty of ±2‰.

In the studies by QTW and TBK the terrestrial biosphere Suess effect ($F_{ab}(R_{ab}^{eq}-R_a)$) has been assumed a magnitude of 12 GtC ‰ yr^{-1}. This value is highly uncertain, for instance, *Enting et al.* [1993] determined a magnitude more than twice as large based on the terrestrial biosphere model of *Emanuel et al.* [1981]. Here we adopt a value of 18 GtC ‰ yr^{-1}. As this parameter basically represents an unknown property we assign it a large uncertainty of 12 GtC ‰ yr^{-1}.

Ocean

All oceanic surface properties which enter the air-sea exchange relations represent global averages weighted with the local gas exchange rate. In general, this em-

phasizes the higher latitudes and the winter season because of the stronger wind speeds. For example, the globally averaged sea surface temperature, weighted by the gas exchange coefficient based on the Liss-Merlivat relationship [*Liss and Merlivat*, 1986], results in 15°C [*Heimann and Monfray*, 1989], which is 4°C lower than the unweighted average of 19°C [*Levitus*, 1982].

The globally integrated gross air-sea exchange flux, based on a bomb-^{14}C derived atmospheric residence time of 7.8 yr [*Siegenthaler*, 1983], is 95 GtC yr^{-1} averaged over 1970–1989. This value is substantially higher than estimates based on direct measurements of the gas exchange coefficient [*Watson*, 1993]. Recent assessments of the global ^{14}C balance indicate a possible need for a downward revision of up to 25% [*Hesshaimer et al.*, 1994; *Broecker and Peng*, 1993]; *Broecker et al.*, 1995. Here we assume an a priori value of 85 GtC yr^{-1} with an uncertainty range of 25%, that is, ±21 GtC yr^{-1}.

Globally averaged surface ocean waters are assigned a DIC concentration of 2.1 mol C m^{-3} with an uncertainty of ±0.05 mol C m^{-3}. The globally averaged buffer factor is 10.5, based on an average sea surface temperature of 15°C, using the chemistry constants given by *Peng et al.*, [1987]. This value is assigned an uncertainty of ±1.

Globally averaged surface water DIC has $^{13}C/^{12}C$ ratios around 1.8‰ [TBK] which is assigned an error estimate of ±0.5‰, subjectively judged from an examination of the data of *Kroopnick* [1985] and as summarized by TBK. The kinetic air-sea fractionation factor, $\alpha_{ma} - 1$, is (at 20°C) -10.3‰ [*Mook*, 1986]. Corrected to a globally averaged ocean temperature of 15°C, this value becomes -10.9‰. *Mook* [1986] assigns an uncertainty estimate of ±0.3‰ to this estimate.

The vertically integrated rate of change of $^{13}C/^{12}C$ in DIC is -10.4‰ m yr^{-1} as determined by QTW. QTW quote an uncertainty estimate of approximately 25% or 2.25‰ m yr^{-1}. This value must represent a lower boundary to the true uncertainty range as it reflects only the statistical error of the regression of the $^{13}C/^{12}C$ measurements with the bomb ^{14}C data. Since the extrapolation to the entire globe relies also on the globally averaged bomb-^{14}C inventory during GEOSECS, which is also uncertain, an additional potential error of up to ±20% must be taken into account. The adopted combined error estimate is thus at least ±30% or 0.30‰ m yr^{-1}.

The globally averaged air-sea isotopic disequilibrium ($R^{eq}_{am} - R_a$) has been determined by TBK as 0.43‰. These authors did not assign a formal error to this number, but discuss a range of possible biases. We believe that this value is uncertain to at least ±0.2‰, primarily because the existing observations of $^{13}C/^{12}C$ ratio of DIC in surface waters are still very sparse and exhibit a large scatter, making a reliable extrapolation to the entire globe difficult. Furthermore, the disequilibrium has to be determined by forming the global average weighted by the local gas exchange rate. The latter presumably may be specified as a function of surface wind speed, the exact form of, however, is still controversial [*Watson*, 1993]. The sensitivity of the determined globally averaged air-sea isotopic disequilibrium with respect to this averaging procedure as quoted TBK of ~0.1‰ must be an underestimate. A similar calculation, based on a seasonal climatology of wind speeds together with their statistical distributions [*Heimann and Monfray*, 1989] indicates that the global air-sea disequilibrium can be shifted by more than 0.4‰ if a uniform gasexchange formulation is replaced by a wind speed dependent formula according to *Liss and Merlivat* [1986]. The Suess effect of oceanic organic carbon $F_{ocb}(R^{eq}_{mb} - R_m)$ is very uncertain. We adopt the value of 5 GtC ‰ yr^{-1} estimated by TBK but assign it an uncertainty of 100%.

River Carbon Fluxes

As discussed in section 2, we assume a steady state with respect to the river carbon transport fluxes. Organic carbon transported into the ocean by rivers in dissolved and particulate forms is assumed to be 0.4 ± 0.3 GtC yr^{-1}, and river transport of inorganic carbon is assumed as 0.4 ± 0.2 GtC yr^{-1} based on the compilation by *Sarmiento and Sundquist* [1992]. In the present calculations, half of the inorganic river carbon transport is assumed to come from CO_2 in soils with an isotopic ratio of approximately -20 ‰ [*Cerling*, 1984]. The other half of the inorganic river carbon flux is assumed to come from carbonate rocks with an isotopic ratio of approximately 0 ‰, hence the average isotopic composition of inorganic river carbon would be -10 ‰ [*Mook*, 1986].

Acknowledgments. We thank Wallace Broecker and the late Uli Siegenthaler for many stimulating discussions. We are also grateful to the reviewers Ralf Keeling and Pieter Tans for clarifying remarks regarding the role of the rivers. This work has been supported by the Commission of the European Union under contract EPOC-CT90-0017.

References

Andres, J.J., G. Marland, T. Boden, and S. Bischoff, Carbon dioxide emissions from fossil fuel consumption and cement manufacture 1751 to 1991 and an estimate for their isotopic composition and latitudinal distribution, in *The Carbon Cycle*, edited by T. M . L. Wigely, Cambridge University Press, New York, in press, 1996.

Bacastow, R.B., and E. Maier-Reimer, Ocean circulation model of the carbon cycle, *Clim. Dyn., 4,* 95-126, 1990.

Barnola, J.-M., M. Anklin, J. Porcheron, D. Raynaud, J. Schwander, and B. Stauffer, CO_2 evolution during the last millenium as recorded by Antarctic and Greenland ice, *Tellus, 47B,* 264–272, 1995.

Broecker, W.S., and T.-H. Peng, *Tracers in the Sea*, Eldigio, Lamont Doherty Geological Observatory, Palisades, New York, 1982.

Broecker, W.S., T.-H. Peng, G. Östlund, and M. Stuiver, The distribution of bomb-radiocarbon in the ocean, *J. Geophys. Res., 90*, 6953–6970, 1985.

Broecker, W.S., Keeping global change honest, *Global Biogeochem. Cycles, 5*, 191–192, 1991.

Broecker, W.S., and T.-H. Peng, Evaluation of the ^{13}C constraint on the uptake of fossil fuel CO_2 by the ocean, *Global Biogeochem. Cycles, 7*, 619–626, 1993.

Broecker, W.S., W. Sutherland, W. Smethie, T.-H. Peng, and G. Ostlund, Oceanic radiocarbon: Separation of the natural and bomb components, *Global Biogeochem. Cycles, 9*, 263–288, 1995.

Cerling, Th.E., The stable isotopic composition of modern soil carbonate and its relationship to climate, *Earth Planet. Sci. Lett., 71*, 229–240, 1984.

Degens, E. T., S. Kempe and J. E. Richey, Summary: Biogeochemistry of major world rivers, in *Biogeochemistry of Major World Rivers*, edited by E. T. Degens, S. Kempe and J. E. Richey, *SCOPE Rep. 42*, John Wiley, New York, 1991.

Emanuel, W.R., G.E.G. Killough, and J. S. Olson, Modelling the circulation of carbon in the world's terrestrial ecosystems, in *Carbon Cycle Modelling*, edited by B. Bolin, *SCOPE Rep. 16*, pp. 335–364, John Wiley, New York, 1981.

Enting, I.G., C. M. Trudinger, R. J. Francey, and H. Granek, Synthesis inversion of atmospheric CO_2 using the GISS tracer transport model, *Tech. Pap. No. 29*, CSIRO, Div. of Atmos. Res., Melbourne, Australia, 1993.

Enting, I. G., T. M. L. Wigley and M. Heimann, Future emissions and concentrations of carbon dioxide: Key ocean/atmosphere/land analyses, *Tech. Pap. No. 31*, CSIRO, Div. of Atmos. Res., Melbourne, Australia, 1994.

Etheridge, D. M. et al., Major changes in the growth rate of atmospheric CO_2 over the last 600 years from air in ice and firn from Law Dome, Antarctica, *J. Geophys. Res.*, in press, 1996.

Friedli, H., H. Lötscher, H. Oeschger, U. Siegenthaler, and B. Stauffer, Ice record of the $^{13}C/^{12}C$ ratio of atmospheric CO_2 in the past two centuries, *Nature, 324*, 237–238, 1986.

Harrison, K., W.S. Broecker, and G. Bonani, A strategy for estimating the impact of CO_2 fertilization on soil carbon storage, *Global Biogeochem. Cycles, 7*, 69–80, 1993.

Heimann M. and P. Monfray, Spatial and temporal variation of the gas exchange coefficient for CO_2, 1, Data analysis and global validation. *Rep. No. 31*, Max-Planck-Institut für Meteorologie, Hamburg, Germany, 1989.

Hesshaimer, V., M. Heimann, and I. Levin, Radiocarbon evidence for a smaller oceanic carbon dioxide sink than previously believed, *Nature, 370*, 201–203, 1994.

Keeling, C. D., The Suess Effect: ^{13}Carbon-^{14}Carbon interrelations, *Environ. Int., 2*, 229–300, 1980.

Keeling, C. D., R. B. Bacastow, A. F. Carter, S. C. Piper, T. P. Whorf, M. Heimann, W. G. Mook, and H. Roeloffzen, A three dimensional model of atmospheric CO_2 transport based on observed winds, 1, Analysis of observational data, in *Aspects of Climate Variability in the Pacific and the Western Americas*, edited by D. H. Peterson, pp. 165–236, AGU, Washington D. C., 1989.

Keeling, C. D., T. P. Whorf, M. Whalen, and J. van der Plicht, Interannual extremes in the carbon dioxide since 1980, *Nature, 375*, 666–670, 1995.

Kroopnick, P.M., The distribution of ^{13}C of ΣCO_2 in the world oceans, *Deep Sea Res., 32*, 57–84, 1985.

Leuenberger, M., U. Siegenthaler and C.C. Langway, Carbon isotope composition of atmospheric CO_2 during the last ice age from an Antarctic ice core, *Nature, 357*, 488–490, 1992.

Levitus, S., Climatological atlas of the world ocean, pp. 173, *NOAA Prof. Pap. 13*, Rockville, Md., 1982.

Liss, P., and L. Merlivat, Air-sea gas exchange rates: Introduction and synthesis, in: *The Role of Air-Sea Exchange in Geochemical Cycling*, edited by P. Buat-Menard, pp. 113, D. Reidel, Norwell, Mass., 1986.

Maier-Reimer, E., Geochemical cycles in an ocean general circulation model, Preindustrial tracer distributions, *Global Biogeochem. Cycles, 7*, 645–678, 1993.

Maier-Reimer, E., and K. Hasselmann, Transport and storage of CO_2 in the ocean — an inorganic ocean-circulation carbon cycle model, *Clim. Dyn., 2*, 63–90, 1987.

Maier-Reimer, E., and R. B. Bacastow, Modelling of geochemical tracers in the ocean, in *Climate-Ocean Interaction*, edited by M. E. Schlesinger, pp. 233–267, Kluwer Academic, Norwell, Mass., 1990.

Maier-Reimer, E., U. Mikolajewicz, and K. Hasselmann, Mean circulation of the Hamburg LSG OGCM and its sensitivity to the thermohaline surface forcing, *J. Phys. Oceanogr., 23*, 731–757, 1993.

Marland, G., and T. Boden, The magnitude and distribution of fossil-fuel-related carbon releases, in: *The Global Carbon Cycle*, edited by M. Heimann, pp. 117–138, Springer-Verlag, Berlin, 1993.

Marland, G., and R. M. Rotty, Carbon dioxide emissions from fossil fuels: A procedure for estimation and results for 1950–1982, *Tellus, 36B*, 232–261, 1984.

Mook, W. G., J. C. Bommerson, and W. H. Staverman, Carbon isotope fractionation betwen dissolved bicarbonate and gaseous carbon dioxide, *Earth Planet. Sci. Lett., 22*, 169-176, 1974.

Mook, W. G., ^{13}C in atmospheric CO_2, *Neth. J. of Sea Res., 20*, 211–223, 1986.

Nydal, R., and K. Lovseth, Tracing bomb ^{14}C in the atmosphere, *J. Geophys. Res., 88*, 3621–3646, 1983.

Oeschger, H., U. Siegenthaler, U. Schotterer, and A. Gugelmann, A box diffusion model to study the carbon dioxide exchange in nature, *Tellus 27*, 168–192, 1975.

Peng, T.-H., T. Takahashi, W. S. Broecker, and J. Olafsson, Seasonal variability of carbon dioxide, nutrients and oxygen in the northern North Atlantic surface water: Observations and a model, *Tellus, 39B*, 439–458, 1987.

Quay, P. D., B. Tilbrook, and C. S. Wong, Oceanic uptake of fossil fuel CO_2: Carbon-13 evidence, *Science, 256*, 74–79, 1992.

Sarmiento, J. L., and E. T. Sundquist, Revised budget for the oceanic uptake of anthropogenic carbon dioxide, *Nature, 356*, 589–593, 1992.

Sarmiento, J. L., J. C. Orr, and U. Siegenthaler, A perturbation simulation of CO_2 uptake in an ocean general circulation model, *J. Geophys. Res. 97*, 3621–3645, 1992.

Schimel, D., I. Enting, M. Heimann, T. Wigley, D. Raynaud, D. Alves, and U. Siegenthaler, The global carbon cycle, in *Radiative Forcing of Climate Change, Report to IPCC from the Scientific Assessment Working Group (WGI)*, edited by J. Houghton et al., pp. 35–71, Cambridge University Press, New York, 1995.

Siegenthaler, U., Uptake of excess CO_2 by an outcrop-diffusion model of the ocean, *J. Geophys. Res., 88*, 3599–3608, 1983.

Siegenthaler, U., and H. Oeschger, Biospheric CO_2 sources emissions during the past 200 years reconstructed by deconvolution of ice core data, *Tellus, 39B*, 140–154, 1987.

Siegenthaler, U., and J. L. Sarmiento, Atmospheric carbon dioxide and the ocean, *Nature, 365*, 119–125, 1993.

Stuiver, M., and P. D. Quay, Atmospheric ^{14}C changes resulting from fossil fuel CO_2 release and cosmic ray flux variability, *Earth Planet. Sci. Lett., 53*, 349–362, 1981.

Tans, P. P., On calculating the transfer of carbon-13 in reservoir models of the carbon cycle, *Tellus, 32*, 464–469, 1980.

Tans, P.P., J. A. Berry, and R. F. Keeling, Oceanic $^{13}C/^{12}C$ observations: A new window on ocean CO_2 uptake, *Global Biogeochem. Cycles, 7*, 353–368, 1993.

Tarantola, A., and B. Valette, Generalized nonlinear inverse problems solved using the least squares criterion, *Rev. Geophys., 20*, 219–232, 1982.

Toggweiler, J. R., K. Dixon, and K. Bryan, Simulations of radiocarbon in a coarse-resolution world ocean model, 2, Distributions of bomb-produced carbon 14, *J. Geophys. Res., 94*, 8243–8264, 1989.

Wanninkhof, R., Relationship between wind speed and gas exchange over the ocean, *J. Geophys. Res., 97*, 7373–7382, 1992.

Watson, A., Air-sea gasexchange and carbon dioxide, in: *The Global Carbon Cycle*, edited by M. Heimann, pp. 397–412, Springer-Verlag, Berlin, 1993.

Winguth, A., M. Heimann, K. D. Kurz, E. Maier-Reimer, U. Mikolajewicz, and J. Segschneider, El Niño-Southern Oscillation related fluctuations of the marine carbon cycle, *Global Biogeochem. Cycles, 8*, 39–63, 1994.

Woodruff, S. D., R. J. Slutz, R. L. Jenne, and P. M. Steurer, A comprehensive ocean-atmosphere data set, *Bull. Am. Meteorol. Soc., 68*, 1239–1250, 1987.

M. Heimann and E. Maier-Reimer, Max-Planck-Institute für Meteorologie, Bundesstraße 55, D-20146, Hamburg, Germany. (e-mail: heimann@dkrz.de; maier-reimer@dkrz.de)

(Received November 22, 1994; revised October 11, 1995; accepted October 17, 1995.)